UNIVERSITY OF OKLAHOMA

GRADUATE COLLEGE

DISCOVERY OF THE MOLECULAR INTERACTIONS MEDIATING MALARIA TRANSMISSION IN THE MOSQUITO MIDGUT

A DISSERTATION

SUBMITTED TO THE GRADUATE FACULTY

in partial fulfillment of the requirements for the

Degree of

DOCTOR OF PHILOSOPHY

By

GENWEI ZHANG
Norman, Oklahoma
2017

DISCOVERY OF THE MOLECULAR INTERACTIONS MEDIATING MALARIA TRANSMISSION IN THE MOSQUITO MIDGUT

A DISSERTATION APPROVED FOR THE
DEPARTMENT OF CHEMISTRY AND BIOCHEMISTRY

BY

_____
Dr. Jun Li, Chair

_____
Dr. Ann H. West

_____
Dr. Christina Bourne

_____
Dr. Zhibo Yang

_____
Dr. David S. Durica

I dedicated this work to my parents, Jixing Zhang and Huanju Ma, neither of whom received higher education, but unconditionally directed and taught me how to behave towards the path to knowledge and truth.

Finally, I would like to acknowledge my wife, Nanxi Li, who continuously supports and encourages me over time. I will keep praying for our harmonious union.

Acknowledgements

Here and now, I want to express my sincere gratitude to the people that have always been important to me, especially to this dissertation.

First of all, I would like to give my top thanks to my advisor, Dr. Jun Li for his continuing advice and encouragement over the past five years. Without his education and support I would not be who I am today, and this dissertation would not have been completed as what it is now. I believe that his broad knowledge and expertise have benefited me tremendously towards my future career and this Five-year mentorship would impact me profoundly. Moreover, I want to deliver another special thanks to my advisory committee members: Dr. Ann West, Dr. Christina Bourne, Dr. Zhibo Yang and Dr. David Durica for their ceaseless advice and patience. Especially, Dr. Bourne and Dr. Durica invested extra time and efforts into the dissertation revisions, which is greatly appreciated. I also want to thank all the faculty members and staff in the department. My acknowledgement also needs to give to the COBRE that allowed me to use FPLC to determine the oligomerization of FREP1 protein.

Secondly, I want to say thank you so much, Dr. Caio França, for becoming my close fellow graduate student and I know that I will miss all the good times we have had during the past four and half years: eating noodles, attending conferences etc. Thanks to the two postdocs, Dr. Guodong Niu and Dr. Yingjun Cui, for their supervision and technical help throughout my experiments.

Last but not least, I want to thank my parents for nurturing me for these many years and my sister for continuous financial support even after her marriage. More importantly, I thank my wife for showing up in my life as a godsend, and I will always

cherish and protect you as we proceed to this long-life journey together no matter what difficulties and challenges are ahead. Rest your hands on me, and I will bring you to a better life!

Table of Contents

List of Tables

List of Figures

Abstract

Malaria is a worldwide health problem that affects two thirds of the world population and kills approximately one million people annually. Infecting *Anopheline* mosquitoes is the essential step for malaria transmission. However, the molecular mechanisms of *Plasmodium* invasion of the mosquito midgut have not been fully elucidated. We identified that the genetic polymorphisms of fibrinogen-related protein 1 (*FREP1*) gene are significantly associated with *Plasmodium falciparum* infection in *Anopheles gambiae* and essential for *P. berghei* infection in *An. gambiae*. Moreover, we identified that FREP1 was a tetrameric oligomer and secreted outside of cells. Notably FREP1 bound to the mosquito midgut peritrophic matrix (PM) through direct interaction to *Plasmodium* ookinetes that invade mosquitoes. Disrupting FREP1 expression by RNAi or blocking endogenous FREP1 by antibodies significantly ($p \leq 0.01$) inhibited *Plasmodium* infection in mosquito midguts. Based on these, we propose that FREP1 mediates *Plasmodium* invasion of *Anopheles* midguts.

Furthermore, nine *P. berghei* proteins were identified as candidate FREP1 binding partners (FBP) through pull-down experiments followed by mass spectrometry assays. We cloned these genes and expressed them in insect cells and *E. coli*. All insect cell-expressed recombinant FBPs interact with FREP1. To test the role of FBPs in malaria transmission, *E. coli* expressed recombinant proteins were injected into mice to generate polyclonal antibodies. Six FBPs turn out to be strongly immunogenic as evidenced from high specific titers in mouse serum. We will examine activities of these antibodies in inhibiting *P. falciparum* transmission to *An. gambiae in vivo*.

Besides FREP1-mediated pathway, multiple pathways are hypothesized to involving malaria transmission. Through computational approaches based on protein sequences and gene expression profiles, 95 *An. gambiae* genes were selected, and 15 of them were cloned and expressed in insect cells. Ten of the recombinant proteins bound to *Plasmodium* parasites. RNA interference assays confirmed four related to *P. falciparum* transmission to mosquitoes.

Collectively, mosquito midgut FREP1, secreted from the epithelium and functioning as tetramers, mediates *Plasmodium* invasion via anchoring ookinetes to the mosquito PM and facilitates parasite penetration into the epithelium. Our newly identified mosquito midgut proteins including FREP1 and parasitic binding partners will enable us to limit malaria transmission with novel intervention strategies.

Chapter 1 : Introduction

1.1 Life Cycle of Malaria in Mosquitoes

Malaria is an infectious blood disease transmitted through the bite of a mosquito, and a mosquito is the essential vector for malaria transmission. Malaria parasites undergo complex developmental processes in both humans and mosquitoes to complete their life cycles. In the mosquito, malaria transmission begins with genus *Plasmodium*-infected blood from a human host entering into the mosquito midgut[1]. (Fig. 1-1) Within the mosquito midgut, exflagellated male microgametes that formed 30 minutes after temperature decreases[2] and female macrogametes fuse to form diploid zygotes. Surviving zygotes further develop and transform into banana-shaped motile ookinetes that penetrate the mosquito midgut peritrophic matrix (PM) and the midgut epithelium sequentially. After penetration, ookinetes reside between the midgut epithelium and the midgut basal lamina, and grow into sporozoite-producing oocytes. Following the stream of hemolymph, sporozoites reach the mosquito salivary gland, and can be co-injected with the saliva into another human host when the mosquito takes the next blood meal. The dissertation focuses on parasites in mosquitoes.

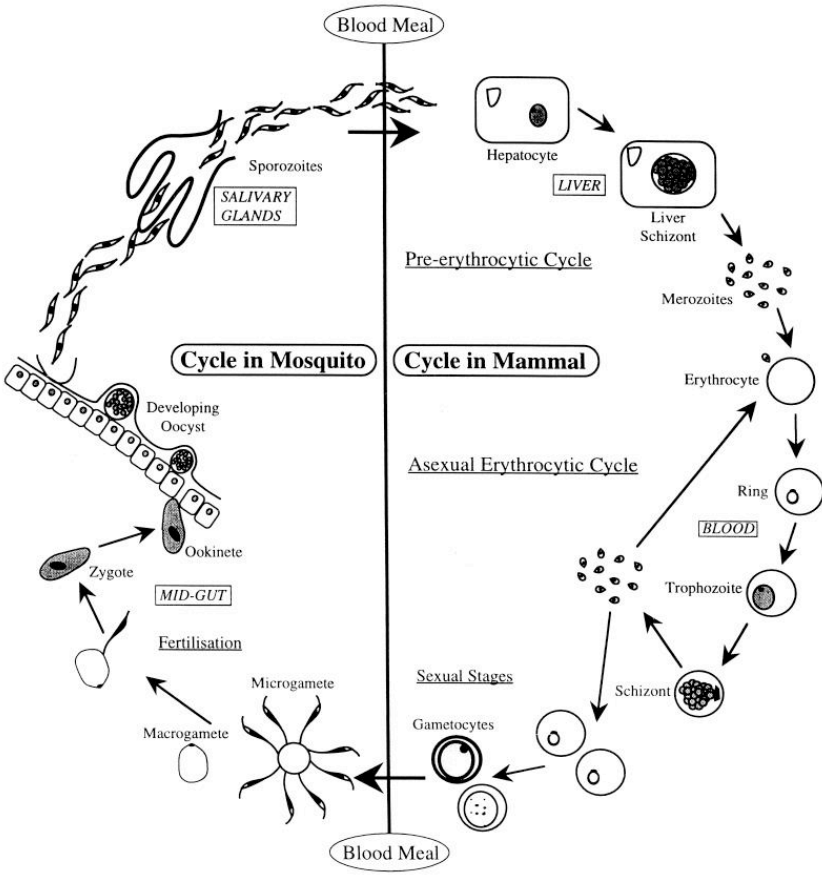

Figure 1-1. The life cycle of the malaria parasites.
[*Clin Microbiol Rev*] REF. 1 © (2001).

1.2 Malaria Infection in Mosquito Midgut

Infecting the mosquito midgut and completing an elaborate developmental course are the mandatory steps for malaria transmission. For millions of years, the co-existence and co-evolution of the malaria parasites and mosquitoes indicate that mosquito has been selected as an optimal host by the malaria parasites over time. It's well known from genetic and genomic analyses that host-pathogen molecular interactions are involved in the processes of malaria parasites invading and infecting mosquitoes [3, 4].

1.2.1 *Plasmodium* Survival in the Mosquito Midgut Lumen

The mosquito midgut lumen, the first contact of malaria parasites in the mosquito, presents a hostile environment for malaria parasties, due to the presence of diverse digestive enzymes secreted from the mosquito midgut after a blood meal and the high luminal pH [5]. But as an evasive strategy, the parasites located within the center of the blood bolus may remain sufficiently protected with enough time to develop into enzyme-nonsusceptible ookinetes comparing to parasites located close to the periphery of the blood bolus [6]. However, not many studies regarding parasites and mosquito molecular interactions have been reported [7].

Once malaria parasites develop into ookinetes, they need to escape from the blood bolus and invade midguts. One proposed mechanism is that plasminogen, captured by ookinete surface-expressed enolase, is converted to active plasmin, which can then act as a serine protease to dissolve fibrin blood clots and facilitate parasite escape from the blood bolus [8]. The interaction between enolase and plasminogen is mediated by a unique six amino acid lysine motif in enolase recognizing the Kringle domains of plasminogen. The deletion of this interaction leads to a strong inhibition of oocyst formation, confirmed the essential role of enolase and plasmingogen for the parasite development in the mosquito [8].

1.2.2 Mosquito Midgut PM Barrier

The peritrophic matrix (PM), a non-cellular chitin-containing membrane, is formed by secretory materials including chitin from mosquito epithelial cells after a blood meal and envelops blood in the midgut. The PM becomes distended by the ingested blood meal, constructing one of the major physical barriers to ookinetes

invasion. In order to cross the PM, the ookinetes secrete chitinase that digests the chitin-containing PM, creating an opening to help invasion [9, 10]. However, other hydrolytic enzymes, aside from chitinase may also participate in this process [6]. As part of my dissertation work within the group of Dr. Jun Li, the first mosquito PM protein, FREP1, was identified to be involved in the process of ookinete invasion [11]. Using RNA interference-mediated knockdown methods to reduce FREP1 causes a significant reduction in oocysts formation in the mosquito midgut [12].

Although other PM proteoglycans have been proposed to function as recognition sites for *P. falciparum* ookinetes [13], complete mechanisms of mosquito-ookinete interactions remain to be explored and potentially offers additional tools for malaria control.

1.2.3 Penetrating the Mosquito Midgut Epithelium

After parasites overcome the mosquito PM barrier, the malaria ookinetes must cross midgut epithelium. The midgut epithelium surface is lined with mucins, which are composed of complex glycoproteins and carbohydrate molecules. Previous investigations explored interaction between ookinetes and mucin molecules [14, 15]. A mosquito midgut proteoglycan chondroitin sulfate, localized to the microvilli, was found to be essential for *P. falciparum* ookinetes invasion [16]. Further, when the microvillar protein *An. gambiae* aminopeptidase N (AgAPN1) was blocked with antibodies, both *P. berghei* and *P. falciparum* development was strongly inhibited [17]. These studies indicate that the role of microvillar mucins could be anti-malarial targets in blocking the development of malaria parasites within the mosquito host [6].

Parasite-mosquito molecular interactions are involved in parasite penetration of mosquito midgut epithelium [18]. One of the notions would be the observation that feeding the SM1 peptide, a 12-amino acid peptide selected from a phage display library, to mosquitos specifically inhibits the invasion of the midgut epithelium by *P. berghei* ookinetes [19]. Another evidence is that the venom phospholipase A2 strongly inhibits the avian malaria parasite *P. gallinaceum* invasion of mosquito midgut epithelium [20]. Notably, transgenic mosquitoes that synthesize SM1 or phospholipase A2 into the midgut cause severely impaired *Plasmodium* invasion of the midgut [21, 22]. While each of these studies further validates the concept of interfering with parasite invasion by altering or blocking the midgut epithelium molecules, only one example has demonstrated the specific interaction of a malaria parasite ligand (Pvs25) with a mosquito midgut protein (calreticulin) [23]. This highlights a pressing need for further investigations into specific interactions with a long-term aim of halting the malaria cycle at mosquito host invasion.

Many ookinete proteins are also involved in the ookinete invasion process. The reported proteins include CTRP, SOAP, CDPK3, MOAP, PPLP4-5, CelTOS and P28/P25 (Fig. 1-2A). Disruption of a circumsporozoite- and TRAP-related (CTRP) ookinete microneme protein from *P. berghei* shows significant reduced ookinete motility and, consequently, failure of invasion [24]. SOAP, a secreted ookinete adhesive protein, interacts strongly with mosquito laminin in yeast-two-hybrid assays and plays a role in ookinete-to-oocyst differentiation [25]. A *P. berghei* calcium-dependent protein kinase (CDPK3) regulates the ookinete access to and penetration of the midgut epithelial cell [26]. *P. berghei* membrane-attack ookinete protein, MOAP, plays an

essential role in ookinete midgut invasion as evidenced by a loss of midgut infectivity after MAOP gene disruption [27]. Similar to MOAP, perforin-like proteins 4 (PPLP4) from *P. falciparum* and PPLP5 from *P. berghei* have also been found to be required for mosquito midgut invasion in *Anopheles stephensi* and *An. gambiae,* respectively [28, 29]. Targeted disruption of a novel cell-traversal protein for ookinetes and sporozoites (CelTOS) reduced parasites infectivity in mosquito hosts by approximately 200 folds [30]. By using single and double knockouts of *P. berghei* ookinete surface proteins (P28 and P25), redundant functions of P25 and P28 have been shown previously, but the oocysts transformation in ookinetes lacking both proteins were significantly inhibited [31].

In contrast to parasite proteins, mosquito host proteins required for midgut infection are not well characterized. Previously, only a few host proteins have been suggested to be involved in the process of ookinetes midgut invasion: annexin-like protein [32], carboxypepetidase B [33], and croquemort scavenger receptor homolog [34]. Therefore, further investigations for this particular stage are desperately needed for the elucidation of detailed molecular mechanisms.

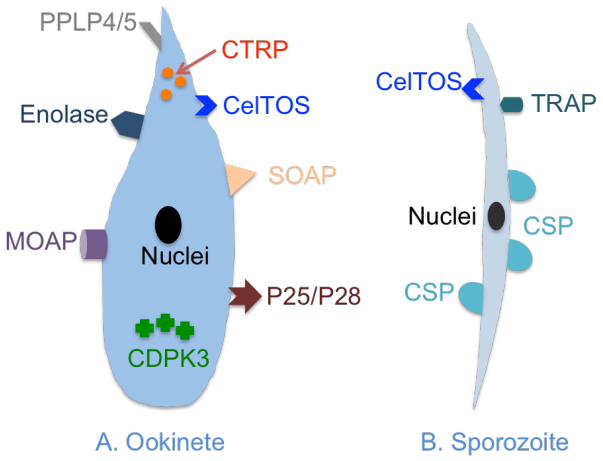

Figure 1-2. Representation of malaria parasite molecules currently implicated infection in mosquito host invasion.
Malaria parasite molecules involved in host mosquito midgut infectivity, as defined in the recent literature (see text). Molecules are listed either on the surface or cytosol for both malaria ookinete (A) and sporozoite (B).

1.2.4 The Mosquito Midgut Basal Side and Anti-*Plasmodium* Defense

To successfully infect the mosquito midgut, malaria parasites need to evade the mosquito's immunosurveillance, especially after penetrating the midgut epithelium. Lacking adaptive immunity, mosquitoes rely on innate immunity for pathogen clearance. Membrane-bound pattern recognition receptors (PPRs) were believed to recognize malaria parasites and mediate downstream immune activation [35], and complement-like defense was considered to be a major mosquito immune response within the hemolymph-circulating system, the hemocoel [35].

The first molecule identified was immune deficiency (IMD) pathway-regulated thioester protein 1 (TEP1), which was suggested to recognize and bind to the ookinetes surface and mark the parasite for lysis and melanization [36]. TEP1 is not alone in this process. Two leucine-rich repeat (LRR) proteins, LRIM1 and APL1, stabilize each other prior to the interaction with TEP1 [37]. Interestingly, another member of LRR

domain-containing protein, LRRD7 (or APL2), has also been shown to have anti-*Plasmodium* activity, although the molecular mechanism has yet been reported [38]. In defense, *P. falciparum* has been reported to take advantage of Pfs47 to evade the mosquito immune system by disrupting JNK signaling, which is a key mediator of antiplasmodial immunity downstream of the PRR activation [39, 40].

Another important mosquito PRR group is the fibrinogen-related protein family (FREP or FBN). As the largest PRR gene family in *An. gambiae* (59 putative members), FREPs have been implicated in mosquito defense rather than blood coagulation. FBN9 has been identified as one of the most potent anti-*Plasmodium* FREP proteins through direct interaction with both *P. berghei* and *P. falciparum* [41]. FBN39, another immunolectin, together with an MD2-like receptor (AgMDL1) have been shown to influence mosquito resistance to malaria, but specifically in regulating only resistance to *P. falciparum* [38]. A polymorphism within FBN30, also known as FREP8, has also been linked to the inhibition of *An. gambiae* parasite infection through genome-wide association studies [11].

Melanization, as a ubiquitous insect immune response, is utilized by mosquitoes for anti-*Plasmodium* defense [42]. Melanizing malaria parasites is one big component of host innate immunity. After being melanized, malaria ookinetes are isolated from their surroundings and eventually undergo lysis. However, a mosquito C-type lectin, CTL4, has been shown to facilitate the development of *P. berghei* in *An. gambaie* through inhibiting melanization [43].

Interestingly, studies on serine protease inhibitors (serpins, SRPN) identified two proteins, SRPN2 and SRPN6, which showed complete opposite functions. SRPN2

can facilitate midgut invasion by the malaria parasite *P. berghei* [44], in contrast, SRPN6 as an immune responsive protein was found to mediate mosquito defense against malaria parasites [45].

1.3 Malaria Vector Control

Malaria transmission requires mosquitoes as a vector to progress through the parasite life cycles. Malaria intervention strategies have identified that mosquito midgut infection is a major bottleneck for malaria transmission [46]. While developing within mosquito midgut, malaria parasites encounter significant challenges, including physical barriers, mosquito active immune responses, digestive enzymes, and residing gut microbiota. These factors result in a thousand-fold reduction of parasites [35] (Fig. 1-3). This bottleneck during midgut mosquito infection has been used to develop anti-malaria strategies.

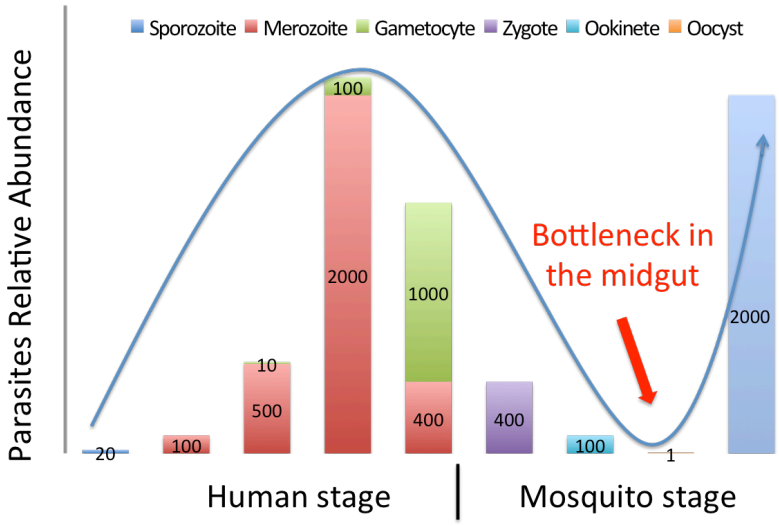

Figure 1-3. Bottleneck of malaria transmission in mosquito midgut.
Malaria parasites encounter a severe bottleneck in the mosquito midgut during the transmission cycle. Numbers shown in the figure are relative parasite quantification based on a previously published paper [18].

1.3.1 Anti-Malarial Drug Development and Issues

The traditional approach to develop anti-malarial drugs is to target parasites in malaria patients. The two most pervasive antimalarial drugs are artemisinin and chloroquine. Both drugs inhibit parasite growth through blockage of utilizing hemoglobin as a nutrient. However, the detailed molecular mechanisms of the two drugs still need further investigation [47]. Given the fact that parasites generation passages are fairly fast (typically a couple weeks), the emergence of drug–resistant mutations can be picked up rapidly within the population. Artemisinin resistance in southeast Asia was first reported in 2008 and then subsequently confirmed in other areas [48]. To circumvent this challenge while developing long-lasting and high-efficacy anti-malarial drugs, other novel or combined therapies are required. Developing novel drugs against parasites in humans is challenging due to the significant cost (billions of dollars) and vast timeframe (typically more than a decade). In contrast, the bottleneck of malaria transmission in the mosquito host has been considered a promising target for anti-malaria drug development. Multiple invasion processes in mosquitoes are vital to parasites' survival and consequently proteins responsible for invasion are potential candidate drug targets. These drug-targeting proteins can be categorized based on the 3 stages of the invasion cycle they inhibit: lumen stage, midgut invasion stage, and salivary gland invasion stage.

Since interactions between plasminogen and parasites enolase play critical roles to help parasites escape from the blood bolus, compounds that can disrupt this interaction would possibly sequester the parasites forever inside of the clotted blood and stop transmission at the lumen stage [8]. Targeting the process of ookinete PM invasion,

a fungal library-based high throughput screening study conducted by Prof. Li *et al*. (2015) identified one active antimalarial drug, *p*-orlandin, which reduced the prevalence of *P. falciparum* infection in *An. gambiae* by half with a drug concentration ≥ 8ug/ml [49]. The molecular target of this screening approach is a mosquito midgut PM protein, FREP1, discovered to mediate parasite invasion of the PM [12] (Fig. 1-4). Moreover, as summarized in section 1.2.3, other ookinete surface molecules and/or mosquito proteins showed indispensable roles during parasite midgut epithelium invasion (e. g. chondroitin sulfate, AgAPN1, CTRP, SOAP, CDPK3, MOAP, PPLP4-5, CelTOS, P28/P25, annexin-like protein, carboxypepetidase B); these molecules could also be exploited as potential drug targets. The development of antimalarial drugs that can target different stages of mosquito invasion, however, requires more active investigation.

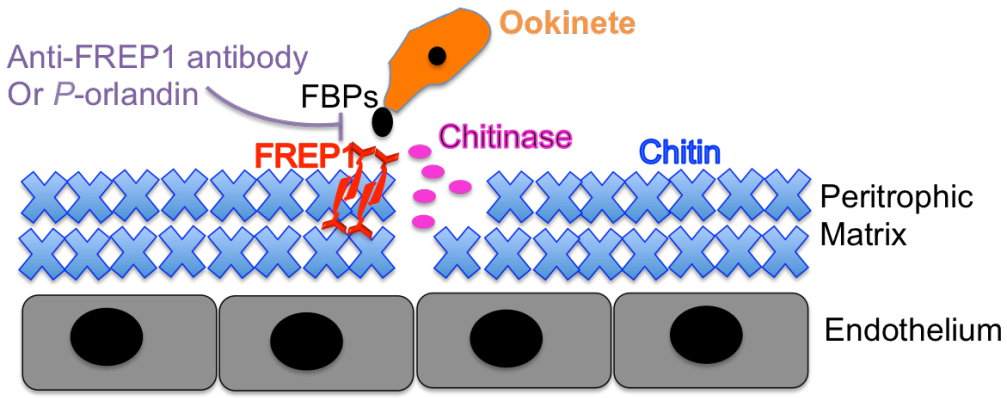

Figure 1-4. Proposed working model to illustrate mosquito midgut FREP1 mediating *Plasmodium* parasites invading the peritrophic matrix (PM).
Invasion of the mosquito midgut by the *Plasmodium* ookinete is mediated by FREP1. Interactions between FREP1 and FBPs can be interrupted by either anti-FREP1 antibodies or *p*-orlandin, suggesting potential mosquito host anti-malarial intervention strategies.
[*J Biol Chem*] REF. 12 © (2015).

Current approaches to antimalarial drugs development include high throughput screening from drug libraries and structure-based drug synthesis/design based on known anti-malarial compounds. Due to the fact that drug chemosynthesis processes typically take years to conduct and evaluate, robot-assisted high throughput technologies have recently been developed. For developing mosquito-based malaria prevention drugs, high throughput techniques would be the mainstream methods and first choice as they are less labor intensive and timesaving. For example, *p*-orlandin discovery process lasted less a year once the mechanism of its target FREP1 was explored [49]. The bases of performing high throughput drug discovery are target identification and selection, where reliability, efficiency and specificity of the interaction must all be evaluated.

1.3.2 Transmission Blocking Vaccine and Obstacles

Vaccines are strong and efficient tools to combat diseases. Numerous efficient vaccines have been developed and have saved billions of human lives. The concept of vaccination was introduced late in the 18th Century; poliovirus and yellow fever vaccines were developed in the 1920s; chickenpox vaccine was developed in the 1950s and hepatitis A/B vaccines were developed during the last half-century (Wikipedia, *Vaccine*). However, there are still many diseases that are difficult to target, for example, no effective vaccine for malaria thus far.

It is very difficult to develop effective malaria vaccines because of its low immunogenicity. Malaria vaccines directed against a single parasites antigen in human hosts are usually less efficient and greater likelihood for acquired resistance [50]. Transmission blocking vaccines (TBV), however, through targeting molecules that are unique to mosquitoes and sexual-stage parasites seems more promising as of the

transmission bottleneck in the mosquito midguts (Fig. 1-3). Antibodies against interacting molecules required for invasion (from mosquito and/or parasites) may block the development or invasion of malaria parasites in the mosquito midguts. FREP1, as the first discovered TBV target in the mosquito midgut PM, has shown its potential as a broad spectrum malaria TBV target after testing its protection of *P. berghei*/*P. falciparum* and *P. vivax* infection on *An. gambiae* and *An. dirus*, respectively [12] (And unpublished data). Other promising TBV targets involving mosquito midgut proteins are SM1/AgAPN1 [17, 51] and carboxypeptidase B [33, 52]. Mice immunized with recombinant *P. falciparum* enolase show protection against parasites infection, indicating enolase can also be exploited as potential protective antigen [53, 54]. Other parasite surface proteins with the prefix pfs or pbs, have been reported as TBV candidates, including a Phase 1 clinical trial Pfs25/Pvs25 [55].

As noted above, vaccines directed against a single midgut antigen may be not enough to completely abrogate parasites. Developing chimeric or poly antigenic targets may therefore prove to be more effective TBV targeting strategies. Sporozoites that evade TBV may multiple rapidly, giving rise to thousands of merozoites in just a few days. Therefore, ideal TBV vaccines would require being safe, efficacious and long-lived, with a lengthy protection time after a single immunization. Although these challenges will not be easy to achieve [50], transmission blocking vaccine development will be a necessary addition to current mechanisms of malaria control.

To summarize, we have seen significant advances in the field of mosquito-based malaria control in terms of both mosquito-malaria interacting molecular mechanisms and the development of intervention strategies. As mechanisms mediating parasite

development in mosquitoes are better understood, the transmission of malaria can be further limited through the combination of both TBVs and anti-malarial drugs. However, it remains too early to be optimistic, as myriad challenges and unforeseen setbacks come along the research road. The main challenge, again, is an incomplete understanding of the molecular interactions between parasites and mosquitoes, which has hindered the progress of malaria control for decades.

Chapter 2 : Mosquito Midgut FREP1 Mediates *Plasmodium* Invasion[†]

2.1 Introduction

Malaria remains a global public health crisis, and *Anopheline* mosquitoes transmit malaria parasites, of which *P. falciparum* is the most dangerous one [56]. Female mosquitoes need to feed on blood for egg production [57]. Feeding on *Plasmodium*-infected blood can result in the ingestion of male and female haploid gametocytes that fuse to form diploid ookinetes, a process that initiates *Plasmodium* infection of the mosquito vector. Ookinetes start invading mosquito midgut epithelial cells between 12 and 24 h after a blood meal feeding [58]. Un-fused gametocytes and ookinetes located near the periphery of the blood bolus in the mosquito midgut are susceptible to attacks by diverse digestive proteases and bacteria [6, 59, 60], whereas gametocytes and ookinetes inside the blood bolus are protected by blood. However, mature ookinetes must cross and exit the blood bolus to initiate invasion of the midgut epithelium. Blood feeding regulates mosquito gene expression [61, 62] and stimulates the formation of the peritrophic matrix (PM) within the midgut [63]. The newly formed PM completely surrounds the ingested blood, separating the blood bolus from secretory midgut epithelial cells, providing a second physical barrier that limits the infection by pathogens co-ingested with the blood meal [64]. The PM is composed of 3–13% chitin microfibrils and is embedded with many known [58] and unknown proteins [65]. Notably, when the ookinetes are mature 12 h after the blood meal [63], the PM also becomes visible in the midgut lumen. To infect mosquitoes, the motile ookinetes must

[†] This work has been published on the Journal of Biological Chemistry. Zhang, G., *et al., Anopheles Midgut FREP1 Mediates Plasmodium Invasion. J Biol Chem*, 2015. **290**(27): p. 16490-501. DOI: 10.1074/jbc.M114.623165.

sequentially attach to and penetrate the PM and the midgut epithelium [18]. At present, the detailed molecular mechanisms involved in ookinete attachment to and penetration of the PM and the subsequent midgut invasion processes are unclear.

We recently identified a mosquito midgut protein, fibrinogen-related protein 1 (FREP1) that is implicated in *Plasmodium* infection in mosquitoes [11]. Specific genetic polymorphisms in *FREP1* are significantly associated with *P. falciparum* infection intensity levels in wild *An. gambiae* populations from Kenya. The FREP1 is a member of the fibrinogen-related protein family (FREPs or FBNs) that contains a highly conserved C-terminal interacting fibrinogen-like (FBN) domain. In vertebrates, fibrinogen molecules usually associate as hexamers and are comprised of two sets of disulfide-bridged α, β, and γ chains that participate as a principal component of both cellular and fluid coagulation [66]. In invertebrates, FREPs/FBNs are common pattern recognition receptors [67, 68] responsible mainly for initiating innate immune responses [69]. For instance, tachylectin proteins in the horseshoe crab regulate host defense by recognizing bacterial lipopolysaccharides [70]. Previous work examining the role and function of FREP/FBN family members in *Anopheles* mosquitoes has shown that two family members, FBN9 and FBN30, appear to restrict *Plasmodium* infection of midgut epithelial cells. Silencing the expression of either FBN9 or FBN30 in mosquitoes increased *Plasmodium* infection [11, 41]. Here, we report the role and function of a third FREP/FBN family member, FREP1, during *P. falciparum* infection of *Anopheles* mosquitoes. Our genetic and biochemical assays reveal that FREP1 functions as a critical molecular anchor in the PM that facilitates *Plasmodium* invasion and infection of mosquito midguts. In contrast to FBN9 and FBN30 that inhibit *Plasmodium*

infection, our results show that FREP1 is an important host factor that promotes infection of mosquito midguts by the major human pathogen, *P. falciparum*. Collectively, our data reveal new insight into *Plasmodium-Anopheles* interactions and identify FREP1 as a promising transmission-blocking target.

2.2 Experimental Procedures

2.2.1 Rearing *An. gambiae* Mosquitoes

An. gambiae G3 strain was maintained at 27°C, 80% humidity with a 12-h day/night cycle. Larvae were reared on ground KOI fish food supplements (~0.1 mg/larvae per day). Adult mosquitoes were maintained with 8% sucrose and fed on ketamine/xylazine-anesthetized mice for egg production.

2.2.2 Expressing Recombinant FREP1 in Insect Cells

The complete FREP1 coding sequence was PCR amplified using primers shown in Table 2-1 from an adult *An. gambiae* cDNA library. Products were cloned into plasmid pIB/V5-His (Life Technologies) to generate pIB-FREP1 (encoding FREP1) and pIB-FREP1-His (encoding FREP1 with a 6×His tag) expression constructs. Constructs were amplified in *E. coli* DH5α and then purified with endotoxin-free plasmid preparation kits (Sigma). Cabbage looper ovarian cell-derived High Five cells [71] were used to express recombinant FREP1 according to the manufacturer's instructions [72]. In brief, endotoxin-free plasmids were mixed with Cellfectin® Reagent (1 μl of Cellfectin/μg of plasmids, Invitrogen) in 5–6 ml of Express Five® SFM medium (Invitrogen). Cells were cultured in 25 cm^2 cell culture flasks (Greiner Bio-One, Monroe, NC) for 48 h at 27°C. Medium and cells were separated by centrifugation at 300 × g for 5 min. The proteins in the medium were concentrated using Amicon®

ULTRA-4 Centrifugal Filter Devices (Milipore, Billerica, MA) by centrifugation at 5,000 × g for 10 min. The 6×His-tagged FREP1 was purified using a Ni-NTA column using a standard protocol [73]. In total, 0.3 mg of insect cell expressed recombinant FREP1 was purified from 50 ml of culture medium with an initial amount of ~1.0 mg of FREP1 in culture supernatant (estimated based on SDS-PAGE). The yield was ~30%.

Table 2-1. FREP1-related PCR primers

Purpose	Primer Name	Primer sequence
In vitro synthesis of *FREP1* dsRNA	Forward	5'- TAATACGACTCACTATAGGAGCTCGAGGTGAAGCAGAG-3'
	Reverse	5'-TAATACGACTCACTATAGGTTCTCCAGCCGGTTGTGT-3'
Verify *FREP1 mRNA* expression	Forward	5'-ACAGGGCAAGTTCGAGAAGA-3'
	Reverse	5'-AAGTCAACCGTACCGTCCTG-3'
AgS7 gene	Forward	5'-GGCGATCATCATCTACGTGC-3'
	Reverse	5'- GTAGCTGCTGCAAACTTCGG-3'
In vitro synthesis of *GFP* dsRNA	Forward	5'-TAATACGACTCACTATAGGCAAGTTTGAAGGTGATACCC-3'
	Reverse	5'-TAATACGACTCACTATAGGCTTTTCGTTGGGATCTTTCG-3'
Clone *FREP1* gene into pQE30	Forward	5'-A*CCCGGG*C*AC*TGCCCTGAACGGTGCAG-3'
	Reverse	5'-GGC*AAGCTT*CGCGAACGTCGGCACAGTC-3'
Clone *FREP1* gene into pIB/V5-His	Forward	5'-TCA*AAGCTT***CACC**ATGGTGAATTCATTCGTGTCG-3'
	Reverse	5'-AC*TCTAGA*TTACGCGAACGTCGGCACAGTCGTG-3'

Note: The italic and underlined sequences are restriction recognition sites. The underlined sequences are T7 promoter. The bold sequence is Kozak consensus sequences.

2.2.3 Gel Filtration Chromatography to Determine the FREP1 Size

Using standard protocols [74], 0.03–1.0 mg of purified High Five-expressed recombinant FREP1 in 0.1 ml of 1×PBS with or without 0.1% Triton X-100 was subjected to fast protein liquid chromatography gel filtration (Bio-Rad). Sephadex G-200 columns (30 cm in length, 1.0 cm in diameter, 5 to 600 kDa resolution) were used with flow rates regulated to 0.2 ml/min. The void volume (V_0) of this column is about 8.0 ml, and the total elution volume (V_t) is about 24.0 ml. Fractions of ~0.1 ml were collected. Absorbance (A280) was monitored constantly, and ELISA was used to detect recombinant FREP1 in each fraction. Briefly, 50 µl of sample from each fraction was coated per well onto an immunoGrade microplate (Brand, Wertheim, Germany) and incubated overnight at 4°C. Wells were blocked for 1.5 h with 100 µl of 1.0% BSA in 1×PBS (BSA-PBS), followed by sequential incubation for 1 h with 100 µl of anti-FREP1 antibody (diluted 5,000-fold in 0.2% BSA-PBS to a concentration of 0.1 µg/ml) and then 1 h in 100 µl of alkaline phosphatase conjugated anti-rabbit IgG (Sigma, 1:20,000 dilution with 0.2% BSA-PBS). Wells were washed three times with PBST (0.2% Tween 20 in 1×PBS) between incubations. Wells were developed with 100 µl of p-nitrophenyl phosphate solution (Sigma). When colors in wells were visible, the optical density absorbance at 405 nm was measured. A set of molecular weight standards was used to establish standard curves of molecular masses for the gel filtration columns (aprotinin (6.5 kDa), ribonuclease A (13.7 kDa), carbonic anhydrase (29 kDa), canalbumin (75 kDa), and ferritin (440 kDa)). The elution (retention) volumes were measured to be 21.05, 18.34, 16.91, 13.65, and 9.38 ml, respectively. The linear regression equation of standard curve based on these standards was y=-6.32x +

44.86, where x is log10 transformed molecular mass in daltons and y is elution volume in milliliters. The correlation coefficient between x and y was 0.99.

2.2.4 Preparation of *P. falciparum* Gametocytes and Ookinetes

P. falciparum parasites (NF54 strain from MR4) were propagated in O^+ fresh human blood (4% red blood cells (RBC), 0.25-0.5% parasitemia). Cultures were maintained in 6-well plates (Corning Inc., Costar) with 5.0 ml of complete RPMI 1640 medium supplemented with 10% heat-inactivated human AB type serum (Interstate blood bank, Memphis, TN) and 12.5 μg/ml of hypoxanthine. The plates were maintained under 37°C in a candle jar [75] and the medium was replaced daily until days 15–17. The parasitemia or gametocytemia was checked every other day by Giemsa staining of thin blood smears. For ookinete enrichment, *P. falciparum* cultures harboring stage V gametocytes were diluted 10-fold in complete RPMI 1640 without sodium bicarbonate and incubated at room temperature for 24 h as described [76]. *P. falciparum* culturing and infection experiments were conducted in the biosafety level 2 (BSL2) laboratory at the University of Oklahoma.

2.2.5 Indirect Immunofluorescence Assays (IFA) to Examine the Binding Between Parasites and Insect Cell-expressed Recombinant FREP1

Standard IFA was performed as described previously [77]. In brief, *P. falciparum* cultures were deposited on coverslips (Fisher Scientific). Cells and parasites were immediately fixed in 4% paraformaldehyde in 1×PBS at room temperature for 30 min, which preserved intact (non-permeabilized) cell membranes. Cells were then sequentially incubated with 100 mM glycine in 1×PBS for 20 min, 0.2% bovine serum albumin (BSA) in 1×PBS for 90 min, High Five cell-expressed FREP1 (10 μg/ml) in

0.2% BSA-PBS for 2 h, enhancer (Alexa Fluor® 594 goat anti-mouse SFX kit, Invitrogen) for 30 min, 5 μg/ml of anti-FREP1 antibody in 1×PBS containing 0.2% BSA for 1 h, and 2 μg/ml of secondary antibody (Alexa Fluor® 594 goat anti-rabbit antibody, in 1×PBS containing 0.2% BSA, Invitrogen) for 30 min in the dark. Between each incubation, the cells were washed 3 times for 3 min in 1×PBS containing 0.2% BSA. Coverslips were rinsed in distilled water for 20 s and mounted on glass slides using 50 μl of Vectashield mounting media (Vector Laboratories, Burlingame, CA). Cell staining was examined using a Nikon Eclipse Ti-S fluorescence microscope. The fluorescence (pixel) intensity was measured as described above. The fluorescence intensity of a target region of an image was calculated by subtracting the mean background fluorescence intensity (gray values) from the mean target fluorescence intensity (gray values). The fluorescence intensity values from three independent experiments or three controls were measured to calculate the mean ± S.D.

2.2.6 Binding Assay Between FREP1 and Midgut PM by ELISA

Three- to five-day-old mosquitoes were fed on anesthetized mice and then maintained with 8% sugar. About 18 h after the blood meal, the engorged mosquitoes were dissected in 1×PBS supplemented with protease inhibitors (PBSI) (Pierce Protease Inhibitor Mini Tablets, EDTA-free, Thermo Scientific, Rock- ford, IL). The blood bolus in each midgut was removed manually. The dissected midguts were washed three times with PBSI. Each replicate contained at least 10 midguts. The same number of unfed (control) mosquito midguts was examined in parallel. Insect cell-expressed recombinant FREP1 (0.75 μg in 100 μl of PBSI) was incubated with experimental and control midguts for 1.5 h. An equivalent amount (0.75 μg in 100 μl of PBSI) of BSA was used

as an additional control. The midguts were then washed three times with PBSI, and shredded with a micro-pestle in PBSI containing 0.5% Tween 20 in 1.5-ml tubes. The insoluble materials were removed by centrifugation at 8,000 × g for 2 min. Supernatants (100 μl) were added into immuno-Grade microplates and the plates were incubated overnight at 4°C. ELISA was used to quantify the relative amount of FREP1 in each reaction.

2.2.7 Ablating FREP1 Expression by dsRNA to Verify Its Function on Susceptibility to *P. falciparum* Infection in *An. gambiae* Mosquitoes

FREP1 was cloned from an *An. gambiae* mosquito cDNA library as described in our previous work [11]. Briefly, nested PCR using the primers listed in Table 2-1 was used to generate a DNA template for synthesis of double-stranded RNA (dsRNA) using the in vitro transcription system T7 Megascript (Amibon, TX). The non-mosquito, negative control sequence was amplified from the Aequoria green fluorescent protein (GFP) gene using the primers listed in Table 2-1. dsRNA was synthesized from these gene fragments using the in vitro transcription system T7 Megascript (Amibon, TX). The FREP1 targeting construct spans a unique sequence from nucleotide 791 to 1,268, corresponding to amino acids 263 to 423 of FREP1. Blast analyses confirmed that no other genes in *An. gambiae* share significant DNA sequence identity with the targeted sequence of FREP1. The dsRNA was purified with a Qiagen RNA purification kit. Approximately 207 ng of dsRNA in a 69 nl solution was injected into the hemocoel of each cold-anesthetized, one-day-old *An. gambiae* G3 female mosquitoes. Approximately 100 mosquitoes per treatment were used for the RNAi knockdown experiments. Thirty-six hours after dsRNA injection, the treated mosquitoes were fed

with *P. falciparum*- infected blood containing 0.2% gametocytes in standard membrane feeding assays [78]. Seven days post-infection and feeding, treated mosquitoes were dissected in 1×PBS and oocysts numbers were counted using light microscopy after staining with 0.1% mercury dibromofluorescein disodium salt in 1×PBS. In the negative control groups, ~100 mosquitoes injected with dsRNA targeting GFP were exposed to the same parasite cultures, and were processed identically to the experimental groups. The transcript knockdown efficiency was confirmed by the quantitative RT-PCR in five treated mosquitoes that were taken randomly 12 h after infection. In parallel, reductions in FREP1 in mosquito midguts were confirmed using immuno-histochemical (IHC) assay, except replacing secondary reagents with Alexa Fluor® 594-conjugated goat anti-rabbit antibody. Fluorescent staining intensity was quantified as described above.

2.2.8 Antibody Blocking Assays of *P. falciparum* Infection in *An. gambiae* Mosquitoes

P. falciparum-infected blood cultures containing mature stage V gametocytes were diluted with the fresh O^+ type human blood to get the 0.2% final concentration of stage V gametocytes. An equal volume of heat-inactivated (65°C for 15 min) AB-type human serum was added. Identical volumes of 1×PBS (1/10 volume of blood) containing different concentrations of rabbit polyclonal anti-FREP1 anti-body (5, 4, 2, 1, and 0.5 mg/ml) were added to the gametocyte cultures. Artificial membrane feeding was conducted using three-day-old female naive mosquitoes. After feeding for 15 min, engorged mosquitoes were separated and maintained with 8% sugar in a BSL2 insectary (28°C, 12-h light/dark cycle, 80% humidity) at the University of Oklahoma. Seven days after infection, midguts were dissected, stained with 0.1% mercury dibromofluorescein

disodium salt in 1×PBS, and examined using light microscopy to count the number of oocysts. Equivalent amounts of purified pre-immune rabbit antibody (Thermo Scientific) were used as controls.

2.3 Results

2.3.1 Recombinant FREP1 Is Secreted from Insect Cells and Forms Tetramers

To begin to understand the basic biochemical characteristics of FREP1, we first examined its functional domains. According to our previous genome annotation [79], full-length FREP1 comprises 738 amino acids, including a 22 amino acid signal peptide at the N terminus, three coiled-coil regions, and a conserved 200 amino acid FBN domain at the C terminus (Fig. 2-1A). All six cysteine amino acid residues are within the C-terminal FBN domain.

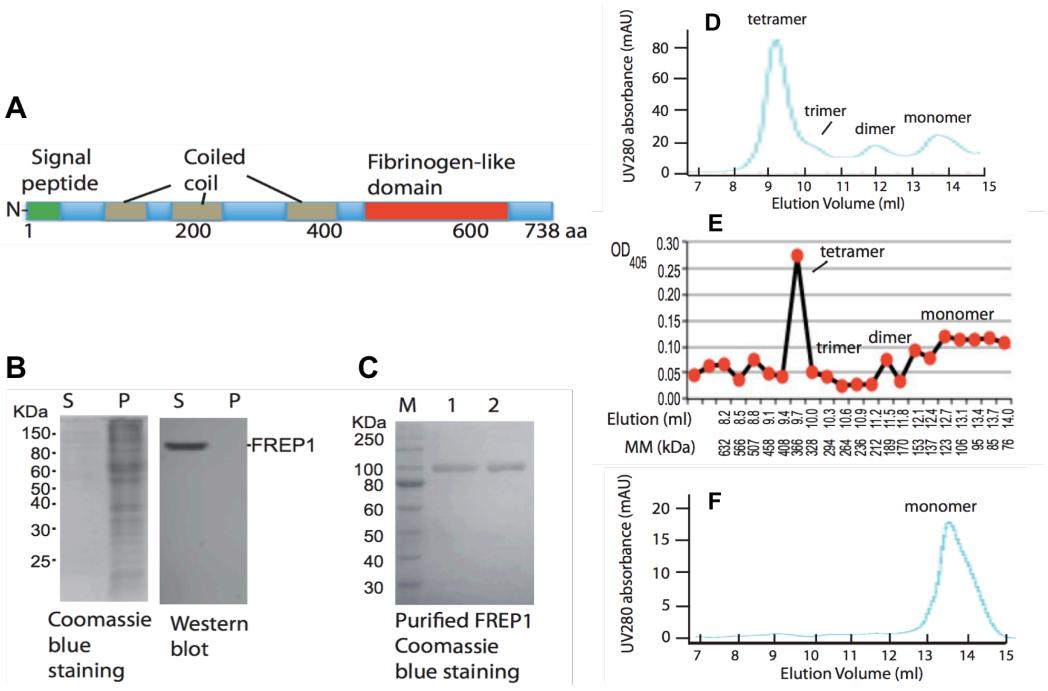

Figure 2-1. FREP1 is secreted from insect cells and forms tetramers.
A, FREP1 has an N-terminal signal peptide, three coiled coils, and a C-terminal FBN

domain. **B**, SDS-PAGE (*left*) and Western blotting (*right*) showing that the recombinant FREP1 is secreted from High Five cells into the culture medium. *S* and *P* represent supernatant and cell pellet and correspond to 1 and 20 μg of protein loaded in gels, respectively. Only one band was detected by anti-FREP1 antibody (0.2 μg/ml). **C**, the purified recombinant FREP1 expressed in High Five insect cells was subjected to reducing (*lane 1*, 1.9 μg of protein) and non-reducing (*lane 2*, 1.9 μg of protein) 12% SDS-PAGE and stained with Coomassie Brilliant Blue. **D**, the UV_{280} absorbance profile of the purified insect cell-expressed recombinant FREP1 in 1×PBS using Sephadex G-200 gel filtration chromatography. **E**, ELISA analysis using anti-FREP1 antibody confirmed that the FREP1 peaks match those identified using gel filtration. The molecular mass (*MM*) were calculated based on the equation of $[(10)]^{((44.86 - y)/6.32)}$, as described under "Experimental Procedures," where *y* is the elution volume in ml. **F**, the UV_{280} absorbance profile of the purified FREP1 in 1×PBS containing 0.1% Triton X-100 using Sephadex G-200 gel filtration chromatography.

We next examined cellular FREP1 expression patterns in vitro. Full-length FREP1 was expressed in High Five insect cells as described under "Experimental Procedures." We found that FREP1 was exclusively detected in the cell culture supernatants and absent from the cell pellets (Fig. 2-1B), supporting that FREP1 is a secreted protein. Notably, Western blotting using the anti-FREP1 antibody identified only a single band, indicating the anti-FREP1 antibodies recognize FREP1 specifically.

Next we determined whether in vitro-expressed FREP1 form distinct quaternary structures. When supernatants were subjected to SDS-PAGE, the purified insect cell-expressed recombinant FREP1 exhibited identical molecular mass under both reducing (with 2-mercaptoethanol) and non-reducing conditions (Fig. 2-1C), indicating that insect cell-expressed recombinant FREP1 exists as either monomers or multimers that associate via non-covalent bonds. The observed molecular mass of insect-expressed recombinant FREP1 (~95 kDa, Fig. 2-1C) is greater than the predicted molecular mass (83.5 kDa), suggesting post-translational modification of secreted FREP1. Gel filtration chromatography was then utilized to separate recombinant FREP1 and protein

complexes, and ELISA was subsequently used to quantify amounts of recombinant FREP1 in each fraction. The profile of UV absorbance at 280 nm from FPLC (Fig. 2-1D) matched the ELISA result (Fig. 2-1E). Based on the gel-filtration standard curves, the dominant recombinant FREP1 peak eluted between 328 and 408 kDa (Fig. 2-1, D and E). Given that the observed molecular mass of recombinant FREP1 is ~95 kDa, these data support that the majority of the secreted, insect cell-expressed FREP1 exists as tetramers (~380 kDa). In addition to monomers and tetramers, FREP1 dimers and trimers were also apparent (Fig. 2-1D). Coiled-coil proteins tend to be elongated and yield aberrant molecular masses when subjected to gel filtration, particularly when the calibration standards are globular proteins. For these reasons, we repeated our gel filtration studies and included a non-ionic detergent to confirm the quaternary structure of the FREP1. We found that addition of 0.1% Triton X-100 to FREP1 eliminated the higher-ordered structures (Fig. 2-1F). To exclude the possibility that the 6×His tag contributed to the formation of FREP1 quaternary structures, we additionally examined highly concentrated, non-tagged recombinant FREP1 in gel-filtration studies. These analyses were consistent with Fig. 2-1E (data not shown). Together, these data show that FREP1 is a secreted mosquito protein that likely forms tetramers through non-covalent hydrophobic interactions.

2.3.2 FREP1 Binds PM

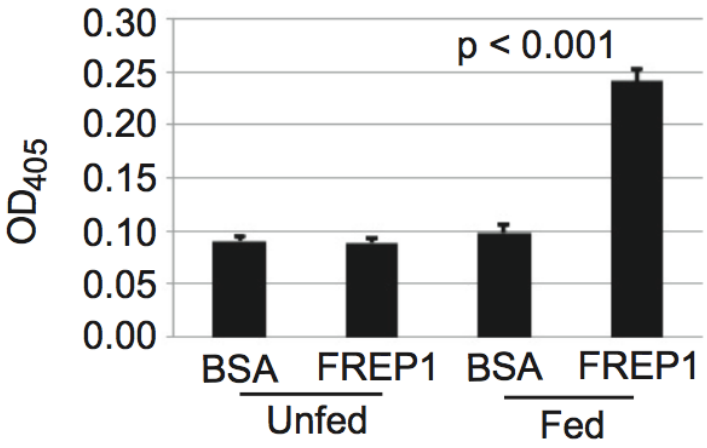

Figure 2-2. Blood-fed mosquito midguts bind FREP1.
Blood-fed mosquito midguts bound significantly ($p < 0.001$) more High Five cell-expressed recombinant FREP1 compared with unfed (naive) mosquito midguts. Purified recombinant FREP1 or irrelevant protein (BSA) was incubated with midguts and the midgut-bound FREP1 was quantified by ELISA. Data (mean ± S.D.) are from three independent experiments.

To verify FREP1 association with the PM, we analyzed the interactions between mosquito midguts and FREP1. The insect cell-expressed recombinant FREP1 was incubated with midguts from naive and blood-fed mosquitoes. The ELISAs were then used to quantify the relative amount of FREP1 that bound midgut preparations. We found that significantly more FREP1 was bound in blood-fed mosquito midguts compared with unfed mosquito midguts ($p < 0.001$, Fig. 2-2). Substituting recombinant FREP1 with BSA eliminated the binding signals. The pattern was consistent in three experiments. Collectively, these results support that FREP1 localizes to and specifically interacts with the mosquito midgut PM.

2.3.3 FREP1 Binds *P. falciparum*

We next sought to determine whether FREP1 could interact with the sexual stage *P. falciparum* parasites. We fixed non-permeabilized *P. falciparum* gametocytes

and ookinetes on coverslips and then probed the cells with insect cell-expressed recombinant FREP1. Anti-FREP1 antibody and fluorescence-conjugated secondary antibodies were used sequentially to determine whether FREP1 bound to gametocytes and ookinetes. In our fluorescence assays, the bound FREP1 appeared red and cell nuclei stained with 4,6-diamidino-2-phenylindole (DAPI) appeared purple. Our results consistently showed that the fluorescence intensity of *P. falciparum* gametocytes (Fig. 2-3, row B) and ookinetes (Fig. 2-3, row C) were significantly ($p<0.01$) higher than those of healthy (non-infected) human RBC (Fig. 2-3, row A), supporting that the recombinant FREP1 can specifically bind both sexual stage (gametocytes) and mosquito midgut stage (ookinetes) *P. falciparum*. Of note, non-infected RBCs do not contain nuclei and are therefore not stained by DAPI. To confirm that addition of FREP1 is necessary to generate the signals in the IFA assays, we performed the same experiments omitting FREP1 and using only secondary reagents (Fig. 2-3, rows D and E). The absence of the detectable fluorescence signal further supports that FREP1 binds to the sexual stage of *P. falciparum* parasites or mosquito invasion stage ookinetes.

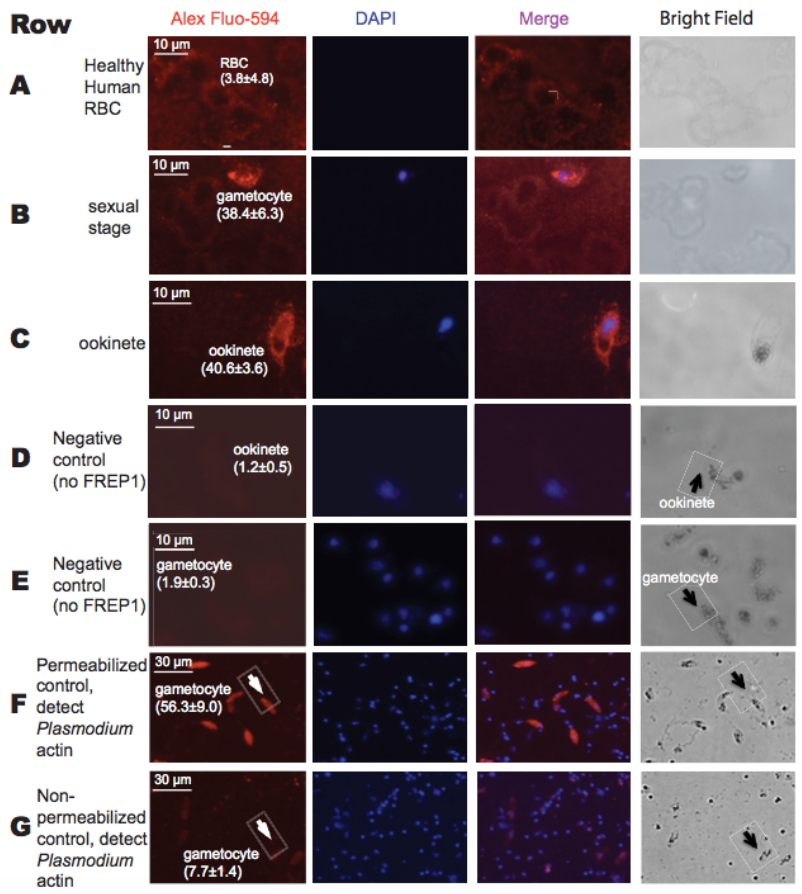

Figure 2-3. Interaction between the recombinant FREP1 and *P. falciparum* demonstrated by immunofluorescence assays.
Images in row A depict healthy, non-infected human RBC. Images in rows B and E depict sexual stage gametocytes. Images in the rows C and D are diploid ookinetes. Images in the rows D and E were obtained by conducting the same procedures as rows A–C except no recombinant FREP1 was added. Image F depicts the anti-actin antibody staining of gametocytes that were fixed with 100% methanol. Image G shows that anti-actin antibody does not stain malaria actin within gametocytes that were fixed with 4% paraformaldehyde. Of note, numerous DAPI-positive spots in rows F and G represent extracellular merozoite forms of *P. falciparum*, which become abundantly released after 10 days of culture. The first and second columns depict FREP1 and nuclear staining, respectively. Merging the first and second columns generated the third column. The last column shows cells under bright field. The numbers within parentheses after the cells are the average fluorescence signal intensity values (± S.D.) for three replicates.

Finally, to confirm that our non-permeabilized fixation approaches maintain cell membrane integrity, we stained parasite preparations with antibodies against

Plasmodium actin [80]. Cells containing gametocytes were fixed separately with either 4% paraformaldehyde or 100% methanol on dry ice for 5 min. The results showed that the anti-actin antibody could only stain cells fixed in methanol (Fig. 2-3F), whereas the fluorescence intensity of gametocytes fixed with 4% paraformaldehyde was similar to the background (Fig. 2-3G). Together, these data support that both recombinant FREP1 and anti-FREP1 reagents were reacting extracellularly. Thus, FREP1 binds molecules on the surface of the gametocytes and ookinetes.

2.3.4 Ablating FREP1 Expression Reduced *P. falciparum* Infection

To determine whether FREP1 directly regulates *P. falciparum* infection of *Anopheles* mosquito vectors, we used a standard dsRNA-mediated gene-silencing assay to knockdown FREP1 mRNA in live mosquitoes, and analyzed the impact of this silencing on *P. falciparum* infection of mosquito midguts. One-day-old adult female *An. gambiae* were injected with FREP1 dsRNA and subsequently fed on cultured *P. falciparum* gametocytes 36 h post-dsRNA injection. Because blood meal feeding increases FREP1 expression, we analyzed the efficacy of FREP1 mRNA knockdown 12 h post-blood meal/infection. Quantitative RT-PCR data show that FREP1 dsRNA injection reduced (~20-fold) FREP1 mRNA to nearly undetectable levels 12 h post-blood meal feeding (Fig. 2-4A, lane 2). As a control, we injected mosquitoes in parallel with dsRNA corresponding to an irrelevant target, GFP (Fig. 2-4A, lane 1). Furthermore, the AgS7 gene, which is constitutively expressed in mosquitoes, was used as a control in the quantitative RT-PCR assays (Fig. 2-4A, lanes 3 and 4). We also compared both total protein and FREP1 protein expression levels in control and experimental mosquito midguts using Western blotting and IHC assays. The total

protein concentration and composition in FREP1 dsRNA-treated mosquito midguts (Fig. 2-4B, lane 1) was similar to that of control midguts (Fig. 2-4B, lane 2). However, Western blotting results from five mosquitoes showed that the FREP1 protein was reduced >3-fold in FREP1 dsRNA-treated mosquito midguts, compared with GFP dsRNA-treated mosquito midguts (compare Fig. 2-4C, lanes 1 and 2).

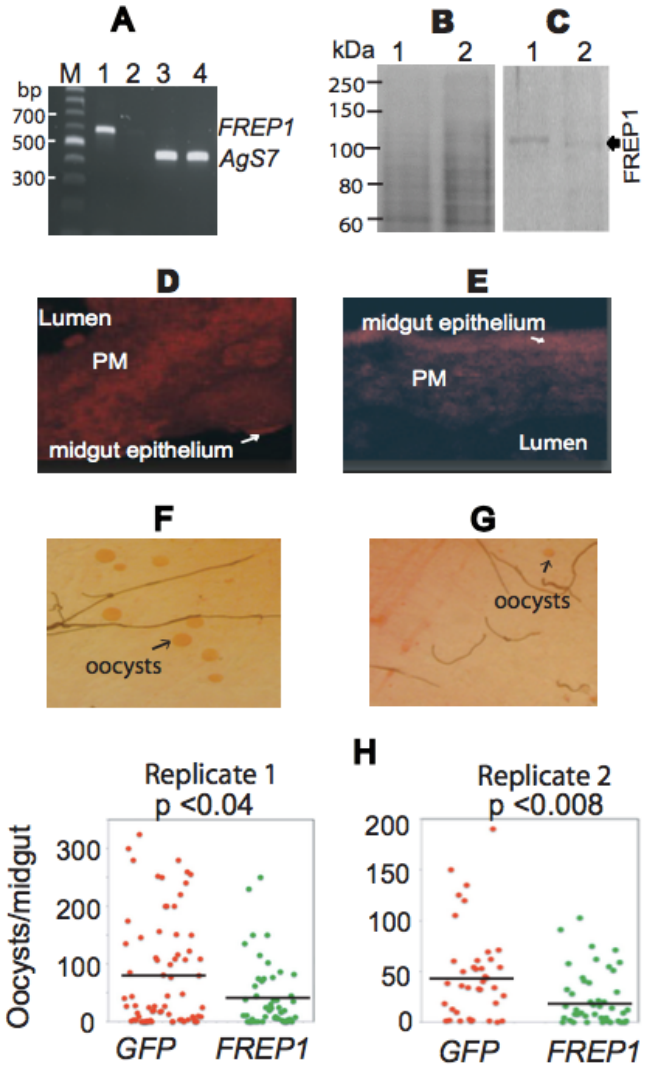

Figure 2-4. Impact of dsRNA-mediated knockdown of *FREP1* on *P. falciparum* infection in mosquitoes.
A, quantitative RT-PCR detection of *FREP1* mRNA in dsRNA-treated experimental and control mosquitoes. Lane order: *M*, DNA ladder; *1*, *FREP1* expression in *GFP* dsRNA-treated mosquitoes; *2*, *FREP1* expression in *FREP1* dsRNA-treated mosquitoes; *3*, *Ags7* expression in *GFP* dsRNA-treated mosquitoes; *4*, *Ags7* expression in *FREP1*

dsRNA-treated mosquitoes. All primer sequences are shown in 2-1. **B**, *GFP* dsRNA-treated (*lane 1*) and *FREP1* dsRNA-treated (*lane 2*) mosquito midgut proteins fractionated on 10% SDS-PAGE and stained with the Coomassie Brilliant Blue. Approximately 10 μg of total protein, extracted from 2 to 3 midguts, was loaded per lane. **C**, gels were loaded as in *B*, and proteins were transferred to membranes and probed with 0.2 μg/ml of anti-FREP1 antibody. *GFP* dsRNA- treated (control, *lane 1*) and *FREP1* dsRNA-treated mosquito (*lane 2*) midgut proteins are shown. The average pixel intensity values of the FREP1 signal in *panel C* are 15.93 and 4.24 for the control and experimental group, respectively. **D** and **E**, immunohistochemical analysis of midgut tissue sections from *GFP* dsRNA-treated (*D*) and *FREP1* dsRNA-treated (*E*) mosquitoes. Sections were probed with anti-FREP1 followed by Alexa Fluor® 594 goat anti-rabbit antibody. The fluorescence intensities of control sections (*D*) were 17.93 ± 1.77, whereas the fluorescence intensities of *FREP1* dsRNA-treated experimental sections (*E*) were 6.32 ± 0.11. The mean fluorescence intensities and standard deviations were obtained from three sections. **F** and **G**, enumeration of oocysts (round red spots) in *GFP* dsRNA-treated (*F*) and *FREP1* dsRNA-treated (*G*) mosquito midguts. **H**, summary data and statistical analyses of the number of oocysts in mosquitoes treated with the dsRNA targeting *GFP* or *FREP1*, respectively. *y* axis represents the number of oocysts per midgut and *x* axis indicates the treatment groups. The *black bars* represent the mean oocysts per midgut. The *p* values between two groups were calculated using Wilcoxon-Mann-Whitney test. Data are representative of two independent experiments.

Given these results, we next examined whether knockdown of FREP1 impacted *P. falciparum* midgut infection. Seven days post-blood meal/infection, we compared the number of oocysts in FREP1 dsRNA-treated and control GFP dsRNA-treated mosquitoes. The data show that significantly ($p < 0.04$) fewer oocysts developed in FREP1-depleted *An. gambiae* midguts (Fig. 2-4G), compared with the GFP dsRNA-treated mosquitoes (Fig. 2-4F). Consistent results were observed in two independent dsRNA-mediated gene expression-silencing experiments (Fig. 2-4H). Together, these data show that FREP1 facilitates *P. falciparum* infection of the *An. gambiae* midgut and the expressed FREP1 in the mosquito midgut PM serves as an agonist for *P. falciparum* invasion.

2.3.5 Anti-FREP1 Antibody Blocks *P. falciparum* Parasite Infection in Mosquitoes

Our data suggest that FREP1 likely exerts its function through direct interaction

with both *Plasmodium* parasites and the mosquito PM. Thus, we hypothesized that interfering with these interactions would inhibit parasite infection of the mosquito midgut. To test this hypothesis, rabbit anti-FREP1 polyclonal antibody was mixed with *P. falciparum* gametocyte cultures (0.2% gametocytes, 0.5 mg/ml of antibody) prior to their use in mosquito membrane feeding-based infection assays. An equivalent amount of purified pre-immune rabbit antibody was used as a negative control. Strikingly, co-ingestion of gametocytes mixed with anti-FREP1 antibody significantly ($p < 10^{-7}$) reduced the number of *P. falciparum* oocysts per midgut by 25- and 60-fold, compared with control antibody-treated cultures in two replicate experiments (Fig. 2-5A). The infection prevalence also decreased from 85 and 82% to 35 and 16%, respectively (Fig. 2-5A). To examine dose-dependent effects of anti-FREP1 antibody on blocking *P. falciparum* infection, we tested a dilution series (0.4, 0.2, 0.1, and 0.05 mg/ml) of antibodies. The results (Fig. 2-5B) show that as the concentration of anti-FREP1 antibody decreased, the number of oocysts in mosquito midguts increased. Notably, antibody concentrations as low as 0.1 mg/ml, which is 5 times lower than the antibody concentration in the original undiluted rabbit serum, still mediated significant ($p < 0.003$) reductions in *Plasmodium* parasite infection in mosquitoes. Thus, vaccination with FREP1 can potentially elicit physiologically relevant titers of anti-FREP1 antibodies capable of exerting transmission-blocking activity in blood feeding mosquitoes.

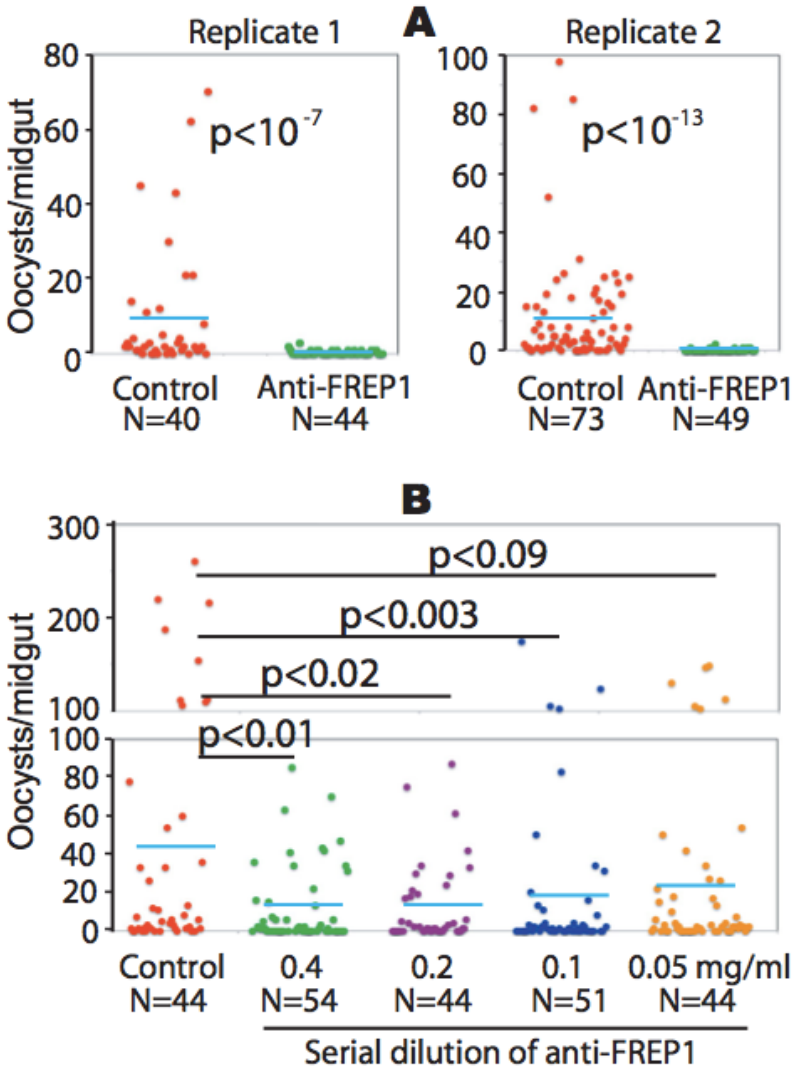

Figure 2-5. The anti-FREP1 antibody blocks *P. falciparum* parasite invasion in mosquitoes.

Three-day-old female *An. gambiae* were fed with *P. falciparum*-infected blood containing 0.2% stage V gametocytes and 0.5 mg/ml of purified anti-FREP1 antibodies (A) or a series of dilutions of anti-FREP1 antibodies (0.4, 0.2, 0.1, and 0.05 mg/ml) (B). Midguts from engorged (fed) mosquitoes were dissected 7 days post-infection and the numbers of oocysts in mosquito midguts were counted microscopically. N represents the number of mosquitoes and the blue bars represent the mean number of oocysts per midgut in each group. Control in panels A and B represent mosquitoes fed on infected blood treated with purified preimmune rabbit antibodies (0.5 and 0.4 mg/ml in A and B, respectively). The *p* values between experimental and the control groups were calculated using Wilcoxon-Mann-Whitney tests. Data represent two independent experiments.

To exclude the possibility that the rabbit anti-FREP1 antibody affected parasite viability before feeding, we examined *P. falciparum* viability following addition of purified anti-FREP1 antibody. Anti-FREP1 was added into cultures at 0.4 mg/ml and an equivalent amount of the purified pre-immune rabbit antibody was used as a control. Twenty-four hours later, the number of *P. falciparum*-infected cells was counted. In three independent experiments we observed equivalent parasitemia (in percentage) in non-treated cultures and cultures containing anti-FREP1 or pre-immune antibody (6.2±0.53, 7.2±0.81, and 6.4±1.32, respectively). No statistical differences in viable parasite numbers were observed among the three groups (p = 0.20). Therefore, anti-FREP1 antibodies do not impact parasite viability outside of the mosquito host. Collectively, these data support that anti-FREP1 antibodies can inhibit *Plasmodium* infection in mosquitoes via disruption of FREP1-parasite interactions within the PM of mosquito midguts.

2.4 Discussion

Based on our experimental data, we propose a molecular model for FREP1 activity during *Plasmodium* invasion (Fig. 2-6). FREP1 is up-regulated and expressed in midguts after a blood meal and our new data support that FREP1 is secreted into the mosquito midgut lumen. In the lumen, the FREP1 may form tetramers through interactions between coiled-coil regions of FREP1 monomers. Our data suggest that FREP1 tetramers are an integral component of the mosquito PM. Thus, FREP1 is likely to be a structural component of the PM, and the tetramerization of FREP1 may perhaps increase the binding affinity between FREP1, the PM, and *Plasmodium* parasites. We speculate that the interactions between ookinetes and FREP1 may facilitate localization

and positioning of ookinetes within the PM, which may further potentiate the enzymatic activities of the chitinase secreted by ookinetes [9]. These interactions and the activity of chitinase, coupled with the digestive activity of plasmin on the ookinete surface [81], may result in a disruption of the PM structure, ultimately facilitating parasite invasion. After ookinetes cross the PM to invade midgut epithelial cells other proteins in mosquito hemolymph may perhaps interact with parasites and impact infection intensity [82, 83].

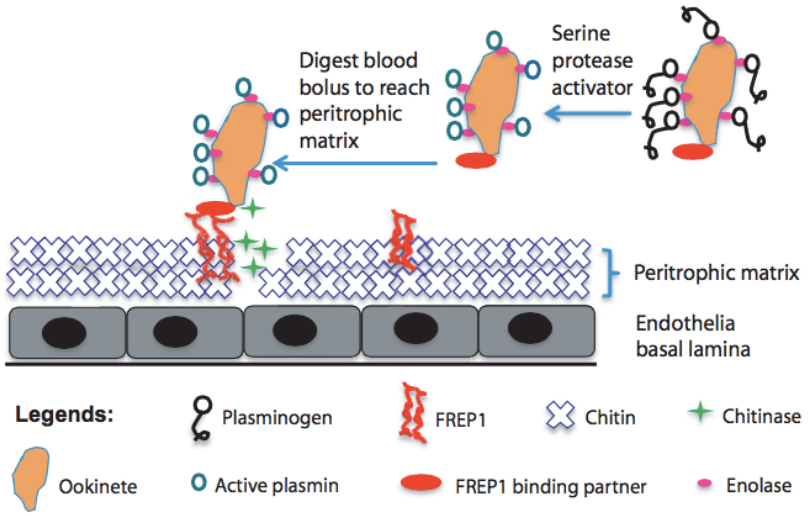

Figure 2-6. Working molecular model for FREP1-mediated *Plasmodium* parasite invasion in *Anopheline* mosquitoes.
After a blood meal, FREP1 is secreted into mosquito midgut lumen and associated with the newly formed PM. PM-associated tetrameric FREP1 binds a putative FREP1-binding partner(s) expressed on the surface of *Plasmodium* parasites, thereby anchoring the parasite within the PM. Stoichiometry of these interactions is under investigation. Continuous secretion of chitinase by anchored ookinetes digests chitin in PM, which results in disruption of PM. Dissolution of the PM enables ookinetes to eventually escape and overcome the PM barrier and subsequently invade the midgut epithelium.

By extension, our model predicts that blocking FREP1 activity or interaction with *Plasmodium* parasites will significantly reduce the capacity for mosquitoes to

transmit malaria. Consistent with this prediction, our published study [11] and new experimental data show that *Plasmodium* infection in mosquitoes is markedly reduced following genetic ablation of FREP1 expression or targeting FREP1 by antibodies. It is worth noting that if the concentration of mature gametocytes in a blood meal is low (i.e. capable of generating less than 100 oocysts per mosquito midgut), blocking FREP1 by RNAi or antibodies rendered the majority of mosquitoes wholly resistant to *P. falciparum* (Fig. 2-5A) and *P. berghei* infection [11]. On the other hand, when the density of gametocytes in blood is high, the infection intensity is still significantly lower in mosquitoes treated with dsRNA (Fig. 2-4H) or anti-FREP1 antibodies, compared with control groups (Fig. 2-5B). Importantly, physiological parasite densities observed in wild *P. falciparum*-infected *An. gambiae* is usually very low, e.g. resulting in less than 10 oocysts per midgut [11]. Thus, FREP1 remains a critical component of pathways for parasite invasion at physiological parasite densities and targeting FREP1 represents a potentially viable strategy to reduce *Plasmodium* transmission.

Ookinetes have to overcome and exit the blood bolus barrier before reaching PM. Previous reports showed that mammalian plasminogen can be captured by enolase on the surface of ookinetes [8]. Plasminogen is an essential serine protease pre-cursor in vertebrate blood. After activation, plasminogen becomes plasmin that can cleave fibrin or fibronectin to free ookinetes in the blood bolus, thereby facilitating their migration to the midgut PM. After traversing the PM, many ookinetes will manage to invade and cross the mosquito midgut epithelium through multiple pathways [84]. Parasite invasion- induced apoptosis of midgut epithelial cells will further determine survival and/or successful ookinete infection [85]. Therefore, interactions between the PM and

Plasmodium parasites (i.e. the "interactome") mediated by FREP1 is important for parasite invasion, and targeting this interaction may prove effective for limiting malaria transmission. It is worth emphasizing that proteins in the PM are readily accessible by antibodies co-ingested after a blood meal [57]. Thus, FREP1 may serve as an excellent potential antigen for inclusion in experimental malaria transmission blocking vaccines. Consistent with this notion, and as we demonstrated in this report, anti-FREP1 antibodies significantly reduced the mosquito vectorial load of malaria parasites. These antibody protection assays further support our proposed molecular model of FREP1 activity during *Plasmodium* invasion.

In summary, here we describe a novel molecular mechanism and function of the mosquito FREP1 during *Plasmodium* infection of the mosquito midgut. We propose that FREP1 acts as an anchor to facilitate ookinete penetration of the PM in mosquito midguts. Consistent with the concept that the PM protects mosquitoes from pathogen infection or invasion, pathogens like *Plasmodium* have also evolved mechanisms to overcome these physical barriers by exploiting the specific constituents of the PM. Understanding the mechanisms of *Plasmodium* parasite invasion of mosquito midguts will identify new opportunities and targets for malaria control.

Chapter 3 : Identification of FREP1 Binding Partner(s) from *P. berghei*

3.1 Introduction

Mosquitoes are the essential vectors for malaria transmission to humans. According to the WHO report in 2016 [86], malaria kills approximately one million people annually, mainly in sub-Sahara Africa. As summarized in Chapter 1, *Plasmodium* parasites have to invade the mosquito midgut epithelium in order to establish an infection in mosquitoes. However, the molecular interactions inside of the mosquito midgut remain largely unknown.

We determined the molecular functions of FREP1, which binds parasites and mediates both *P. berghei* and *P. falciparum* infection in the mosquito midgut peritrophic matrix. However, the FREP1 binding partner(s) (FBPs) in *Plasmodium* have not been identified yet. The goal of this chapter is to identify the binding partner(s) of FREP1 from *P. berghei*.

Since FREP1 binds parasites [12], FBPs might exist on the surface of the parasites. There are three known secretory pathways in *Plasmodium*. In the first pathway, proteins encode a short (5-30 amino acids long) signal peptide to target the protein to the secretory pathway [87]. The fates of these proteins are either secretion from the cell, insertion into cellular membranes or placement within certain organelles (ER, golgi or endosomes) after typical post-translational modifications [87]. In the second mechanism, *Plasmodium* parasites may utilize an unconventional pathway to export proteins onto the host cell surfaces when such proteins contain a *Plasmodium*

export element (PEXEL) motif (a conserved five amino acids sequence, namely RX [L, I] X [D, E, Q]) in the sequence [88]. In the third secretory mechanism, an extended apical pellicle (EP), a large opening required for midgut invasion [89], is formed during ookinete maturation and secretes digestive enzymes like chitinase. Thus, ookinetes harness multiple pathways for secreting proteins, and the identification of more ookinetes surface proteins may lead to a better understanding of *Plasmodium* invasion mechanism.

Previously, several ookinete surface proteins have been characterized and exploited as potential targets for developing anti-malarial tools. The ookinete surface proteins P25/28 and enolase were targeted to develop transmission-blocking vaccines [84, 90]; the *Plasmodium* ookinete apical surface aspartic protease, plasmepsin 4, was also characterized as a potential transmission-blocking target [91].

In this chapter, we identified nine FREP1 binding partner candidates from *P. berghei* lysates using pull-down assays followed by mass spectrometry assays. We cloned these genes from *P. berghei* and expressed them in insect cells and *E. coli*. After immunizing these *E. coli*-expressed recombinant proteins in mice, six proteins show high immunogenicity as measured by mouse serum antibody titers. We are still working on the identification of FBPs.

3.2 Experimental Methods

3.2.1 FREP1 Expression in Insect Cells and Purification Using Ni-NTA

The complete FREP1 coding sequence was PCR amplified using primers as shown in Table 2-1 from an adult *An. gambiae* cDNA library. Products were cloned into plasmid pIB/V5-His (Life Technologies) to generate pIB-FREP1 (encoding FREP1)

and pIB-FREP1-His (encoding FREP1 with a 6×His tag) expression constructs. Constructs were amplified in *E. coli DH5α* and then purified with endotoxin-free plasmid preparation kits (Sigma). Cabbage looper ovarian cell-derived High Five cells [71] were used to express recombinant FREP1 according to the manufacturer's instructions [72]. In brief, endotoxin-free plasmids were mixed with Cellfectin® Reagent (1 µl of Cellfectin/µg of plasmids, Invitrogen) in 5–6 ml of Express Five® SFM medium (Invitrogen). Cells were cultured in 25 cm^2 cell culture flasks (Greiner Bio-One, Monroe, NC) for 48 h at 27°C. Medium and cells were separated by centrifugation at 300 × g for 5 min. The proteins in the medium were concentrated using Amicon® ULTRA-4 Centrifugal Filter Devices (Millipore, Billerica, MA) by centrifugation at 5,000 × g for 10 min. The 6×His-tagged FREP1 was purified using a Ni-NTA column using a standard protocol [73]. In total, the yield was ~30%, as 0.3 mg of insect cell expressed recombinant FREP1 was purified from 50 ml of culture medium with an initial amount of ~1.0 mg of FREP1 present in the culture supernatant (estimated based on SDS-PAGE gel).

3.2.2 Enzyme-linked Immunosorbent Assay (ELISA) to Detect the Interaction Between Recombinant FREP1 and *P. berghei*

P. berghei (ANKA strain) was used to infect mice through i.p. injection. The parasitemia (percentage of the parasite-infected cells) was checked every other day by Giemsa staining on thin blood smears. When the parasitemia reached 10%, gametocytes formation was induced by treating mice with 60 mg phenylhydrazine hydrochloride (Santa Cruz Biotechnology, Dallas, Texas) per Kg body weight (4mg/mL, dissolved in 1×PBS). *P. berghei*-infected red blood cells and uninfected red blood cells were

collected, washed three times with 1 × phosphate buffered saline (1×PBS), and re-suspended in 1×PBS containing 0.2% Tween-20 (PBST). The lysates were prepared by ultrasonication of cells for 10 s 6 times with 50 s intervals on ice, and then centrifuged at 8,000 × g for 5 min to remove intact cells and cellular insoluble aggregates. The proteins in supernatants were used for ELISA assays. A 96-well plate (Brand, Wertheim, Germany) was coated with 2 mg/ml lysates (Measured by Bradford assay) and incubated overnight at 4°C. The next day, each well was then incubated with the following solutions: 1) 200 µL blocking buffer (2 mg/mL BSA in 1×PBS) for 1.5 h; 2) 100 µL recombinant FREP1 protein (100 µg/mL) at RT for 1h; 3) 100 µL of purified anti-FREP1 antibody (1:2,000 dilution with blocking buffer) for 1 h at RT; and 4) 100 µL of alkaline phosphatase-conjugated anti-rabbit IgG (1:20,000 dilution with blocking buffer) for 45 min at RT. The wells were washed with PBST (0.2% Tween-20) three times between incubations. In the end, the plates were developed with 100 µL of *p*-NPP solution (Sigma-Aldrich, St. Luis, MO) until the colors appeared. Finally, the absorbance OD_{405} was measured.

3.2.3 Indirect Immunofluorescence Assay (IFA) to Determine the Interaction Between Recombinant FREP1 and *P. berghei*

Standard IFA was performed as described previously [77]. In brief, *P. berghei* cultures were deposited on coverslips (Fisher Scientific). Cells and parasites were immediately fixed in 4% paraformaldehyde in 1×PBS at room temperature for 30 min, which preserves intact (non-permeabilized) cell membranes. Cells were then sequentially incubated with 1) 100 mM glycine in 1×PBS for 20 min; 2) 0.2% bovine serum albumin (BSA) in 1×PBS (BSA-PBS) for 90 min; 3) High Five cell-expressed

recombinant FREP1 (10 μg/ml) in 0.2% BSA-PBS for 2 h; 4) enhancer (Alexa Fluor® 594 goat anti-mouse SFX kit, Invitrogen) for 30 min; 5) 5 μg/ml of anti-FREP1 antibody in BSA-PBS for 1 h; and 6) 2 μg/ml of secondary antibody (Alexa Fluor® 594 goat anti-rabbit antibody, in BSA-PBS, Invitrogen) for 30 min in the dark. Between incubations, the cells were washed 3 times with BSA-PBS for 3 min each time. Coverslips were rinsed in distilled water for 20 s and mounted onto glass slides using 50 μl of Vectashield mounting media (Vector Laboratories, Burlingame, CA). Cell staining was examined using a Nikon Eclipse Ti-S fluorescence microscope.

3.2.4 FREP1 Immobilization onto Magnetic Support

Three hundreds microliter of N-hydroxysuccinimide (NHS) ester-activated magnetic beads (Thermo Fisher) were placed into a 1.5 mL microcentrifuge tube on a magnetic stand, and the supernatant was discarded after beads immobilization. Beads were then washed with 1 mL of ice-cold 1 mM hydrochloric acid with gentle vortexing for 15 s; the supernatant was discarded, followed by immediate addition of 300 μL of FREP1 (~0.3 mg/ml in 50 mM borate, pH 8.5) with 30 s of gentle vortexing. FREP1 was incubated with the magnetic beads on a rotator for 1.5 h at room temperature (RT). During the first 30 min of the incubation, the tube was vortexed for 15 s every 5 min. For the remaining time, the tube was vortexed for 15 s every 15 min until the incubation was complete. FREP1-coupled magnetic beads were then washed sequentially twice with 1 mL 0.1 M glycine, pH 2.0 for 15 s and one time with 1 mL ultrapure water for 15 s. Lastly, 1 mL of the quenching buffer (3 M ethanolamine, pH 9.0) was added to the beads and the tube was vortexed for 30 s before incubating 2 h at RT on a rotator. After quenching, the FREP1-coupled magnetic beads were stored in 300 μL of the storage

buffer (50 mM borate with 0.05% sodium azide) at 4°C until ready for use. The coupling efficiency was assessed using the Bradford assay measuring the amount of FREP1 protein within the solution before and after coupling.

3.2.5 Pull-down Assay and Quantitative Mass Spectrometry

P. berghei infected cell lysate was incubated with FREP1-coupled magnetic beads at 4°C for 2 h with gentle rotation. The beads were washed 3 times with Pierce™ IP Lysis Buffer (Catalog number: 87787) to remove unbound or weakly bound proteins. Any retained proteins were disrupted from the magnetic beads with 6 M urea, followed by SDS-PAGE analysis to visualize differences in the specific protein bands retained between the control and experimental groups. In the control group, procedures were almost the same as the experimental group except NHS ester-activated magnetic beads quenched with ethanolamine rather than FREP1-coupled magnetic beads were used.

Specific protein bands from the SDS-PAGE gel were excised and analyzed by quantitative mass-spectrometry methods (serviced by Oklahoma State University Proteomics Center). Briefly, the same amount of protein eluted from experimental and control groups were loaded onto the mass spectrometer with three independent replicates. After analyzing the difference of peptide abundance within the eluted samples of the two groups with student's *t*-test, unique proteins in the experimental group were identified.

3.2.6 Baculovirus Expression of Identified FBPs and ELISA Confirmation of the Interactions with FREP1

Oligomers were designed and synthesized (Invitrogen) for identified FBP genes (see Table 3-1), and the coding regions of FBP genes were PCR-amplified from a *P.*

berghei cDNA library. A baculovirus expression system was used for FBP protein expression, following standard procedures [92]. In short, PCR products were digested with restriction enzymes, and ligated into pFastBac1 plasmid (6×His tag was added to the C-terminal of cloned genes). Positive recombinant plasmids were transformed into component *E. coli* DH10Bac strains to generate recombinant bacmids. Positive bacmid-containing colonies were selected by blue-white colony selection. Once bacmids were isolated, the commercially available Sf9 cell line was used for bacmid transfection. Isolated viruses were then used to infect the High-Five insect cell line to generate high-yields of expressed membrane proteins. Three passages later, protein expression was confirmed with ELISA through detecting the 6×His tag at the protein C-terminus. The expression levels of different FBPs in the cell lysate were normalized and then a 96-well plate was coated overnight with 100 µl cell lysate to detect interactions with FREP1. After blocking the plate with 0.2% BSA in 1×PBS, recombinant FREP1 was introduced onto the wells and incubated for 1.5 h with the plate at RT. Purified anti-FREP1 antibody was used to detect any retained FREP1. The plates were developed with 100 µL of *p*-NPP solution (Sigma-Aldrich, St. Luis, MO) until the colors appeared. Finally, the absorbance at 405 nm was measured using plate reader. For the control group, same amount of expressed CAT protein (Chloramphenicol acetyltransferase, containing a 6×His tag at C-terminus) was used to coat plate wells.

Table 3-1. Primers for FBPs expression using baculovirus system.

Gene ID	Primer Name	Primer Sequence
PBANKA_ 1365500	Forward	5'-CGGGATCCATGAAGAAAGGAAATAACG-3'
	Reverse	5'-CGCTCGAGCATAGGTTTTGCTCTAC-3'

PBANKA_0701600	Forward	5’-CGGGATCCATGCCGCAATGGGGGACTGGTA-3’
	Reverse	5’-GCTCTAGAATCCTTTTGATTCATTGGGT-3’
PBANKA_0417700	Forward	5’-CGGGATCCATGAGAGAAGTAATAAGTATAC-3’
	Reverse	5’-GCTCTAGAATAGTCTGCCTCATATCCTTC-3’
PBANKA_1316400	Forward	5’-CGGGATCCATGGAAGAAATGCGATCATTAC-3’
	Reverse	5’-GCTCTAGATCGTCGTCTACTGGATCGATTC-3’
PBANKA_1309700	Forward	5’-CGGGATCCATGAAAGGTTTTAATAATTTTC-3’
	Reverse	5’-GCTCTAGAGTAATATTTATTTCCGCCTC-3’
PBANKA_0711900	Forward	5’-CGGGATCCATGGCTAACGCAAAAGCAAAGC-3’
	Reverse	5’-GCTCTAGAATCAACTTCTTCAACAGTTGGTC-3’
PBANKA_0307800	Forward	5’-CGGGATCCATGAAAGCTGCTAAAAATGAG-3’
	Reverse	5’-GCTCTAGATTCATTCTTTTTCACAG-3’
PBANKA_1133300	Forward	5’-CGGGATCCATGGGAAAAGAAAAAACTCAC-3’
	Reverse	5’-GCTCTAGATTTTTTTGCTGGTGCTTTAGC-3’
PBANKA_1234500	Forward	5’-CGGAATTCATGGCAAAAATTACAAAAATCG-3’
	Reverse	5’-GCTCTAGATTCACCCATTTTATTAAATCCTTC-3’

Note: The underlined sequences are restriction recognition sites.

3.2.7 Anti-FBP Antibody Production in Mouse.

After confirming interactions with FREP1, FBPs were then PCR-amplified with primers (shown in Table 3-2) from the *P. berghei* cDNA library. The sequence-verified PCR products were digested with the corresponding restriction enzymes (can be found in Table 3-2) and the digested products were ligated into the pQE30 expression plasmid and eventually transformed into the *E. coli* M15 strain. Gene expression in *E. coli* M15 transformants was induced with 1 mM isopropyl 1-thio-β-D-galacto-pyranoside (IPTG). After 3-4 h induction at 37°C, cells were pelleted and lysed in buffer B (8 M urea, 100 mM NaH_2PO4 , 10 mM Tris-Cl, pH 8.0). Recombinant FBPs were purified on Ni-NTA column using a standard protocol [73]. 12% SDS-PAGE and Coomassie Brilliant Blue R-250 staining confirmed the purity of recombinant FBPs. Customized polyclonal anti-

FBPs antibodies were generated in mouse by priming the mice with 20 μg purified recombinant FBPs in Complete Freund's Adjuvant (CFA, v/v, 1:1), followed by another two boosts (2 weeks interval) with 20 μg proteins in Incomplete Freund's Adjuvant (IFA, v/v, 1:1). Identical volumes of Buffer B with the same adjuvant as FBP proteins were used as negative immunization controls. ~50 days later, mouse sera were collected. Antibody titer was checked using enzyme-linked immunosorbent assay (ELISA). The 96-well plate was coated with purified FBP antigens prior to probing with serial dilutions of the collected sera. The rest ELISA was subsequently preformed similar to procedures described in section 3.2.6. Equivalent amounts of control mouse serum were used as negative controls.

Table 3-2. Primers for FBPs expression in *E. coli*

Gene ID	Primer Name	Primer Sequence
PBANKA_0701600	Forward	5'-CGGGATCCATGCCGCAATGGGGGACTGGTA-3'
	Reverse	5'-CGCAAGCTTTTAATCCTTTTGATTCATTGGGT-3'
PBANKA_0417700	Forward	5'-CGGGATCCATGAGAGAAGTAATAAGTATAC-3'
	Reverse	5'-GCTCTAGAATAGTCTGCCTCATATCCTTC-3'
PBANKA_1309700	Forward	5'-CGGGATCCATGAAAGGTTTTAATAATTTTC-3'
	Reverse	5'-GCTCTAGAGTAATATTTATTTCCGCCTC-3'
PBANKA_0711900	Forward	5'-CGGGATCCATGGCTAACGCAAAAGCAAAGC-3'
	Reverse	5'-CGCAAGCTTTTAATCAACTTCTTCAACAGTTGGTC-3'
PBANKA_0307800	Forward	5'-CGGGATCCATGAAAGCTGCTAAAAATGAG-3'
	Reverse	5'-CGCAAGCTTTTATTCATTCTTTTTCACAG-3'
PBANKA_1133300	Forward	5'-CGGGATCCATGGGAAAAGAAAAAACTCAC-3'
	Reverse	5'-CGCAAGCTTTTATTTTTTTGCTGGTGCTTTAGC-3'
PBANKA_1234500	Forward	5'- CGGGTCGACTGATGGCAAAAATTACAAAAATCG-3'
	Reverse	5'- CGGAAGCTTTTATTCACCCATTTTATTAAATC-3'

Note: The underlined sequences are restriction recognition sites.

3.3 Results

3.3.1 FREP1 Could Bind *P. berghei* Infected Cells.

Prior to testing *P. berghei* parasites proteins for binding to FREP1 in pull-down assays, we need to confirm FREP1 can interact with the *P. berghei* parasite infected cells in a similar manner to *P. falciparum* (see Chapter 2).

First, an enzyme-linked immunosorbent assay (ELISA) was used to check the interactions between FREP1 and *P. berghei* parasite infected cell lysates. Results show that compared with negative controls, heat-inactivated FREP1 and normal cell culture medium, *P. berghei* infected mouse blood cell lysate containing the sexual stages of the parasite could capture insect cell-expressed recombinant FREP1 (Fig. 3-1A). Furthermore, when a serial dilution of *P. berghei* infected cell lysates were coated onto the plate, decreasing interacting signals were observed, validating that the binding signals were arising from specific interactions of binding between FREP1 and *P. berghei* infected cell lysate, which contains the sexual stages of the parasite (Fig. 3-1B).

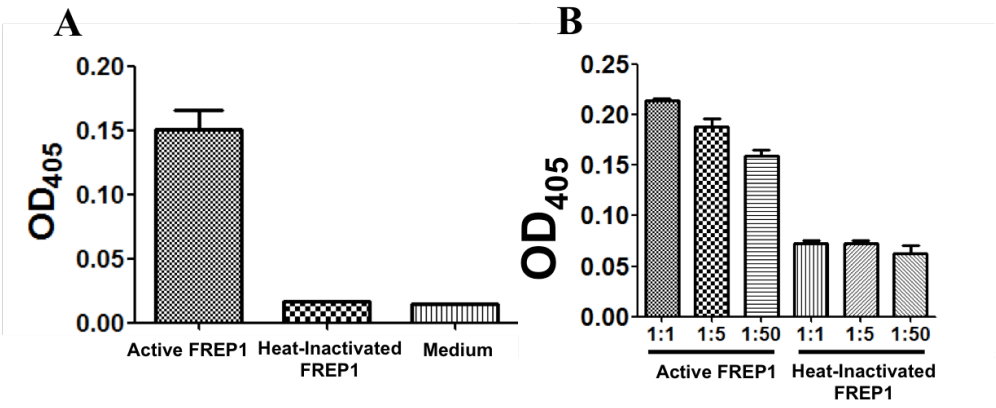

Figure 3-1. ELISA verified that FREP1 interacts with *P. berghei* infected blood cells.
A) *Plasmodium berghei* infected cell lysates were coated onto 96-well plates and incubated with insect cell expressed recombinant FREP1, heat-inactivated FREP1 and normal cell culture medium; B) Serial dilutions of *P. berghei* infected cell lysate was

coated onto 96-well plates, and similar to panel A, heat-inactivated FREP1 was used as negative control. Decreasing trend was observed between the interactions of *P. berghei* infected cell lysate and recombinant FREP1.

Second, we validated the specific binding interaction(s) between FREP1 and *P. berghei* gametocytes and ookines by IFA. We fixed non-permeabilized *P. berghei* gametocytes and ookinetes onto coverslips and then probed the cells with insect cell-expressed purified FREP1. Purified anti-FREP1 antibodies and fluorescence-conjugated secondary antibodies were used sequentially to determine whether FREP1 bound to gametocyte and ookinete surfaces. In our fluorescence assays, the bound FREP1 appeared red and cell nuclei stained with 4,6-diamidino-2-phenylindole (DAPI) appeared purple. Results consistently revealed that the fluorescence intensity of *P. berghei* sexual stage parasites with recombinant FREP1 (Fig. 3-2, row C) were significantly ($p<0.01$) higher than those of healthy (non-infected) mouse red blood cells (RBCs) or parasites without incubation with FREP1 (Fig. 3-2, row A), indicating that the recombinant FREP1 can specifically bind sexual stage *P. berghei*. Of note, non-infected RBCs do not contain nuclei and are therefore not stained by DAPI. Together with the ELISA results, these data consistently support the conclusion that recombinant FREP1 binds *P. berghei* and the potential binding molecules are likely to locate on the surface of the gametocytes and ookinetes.

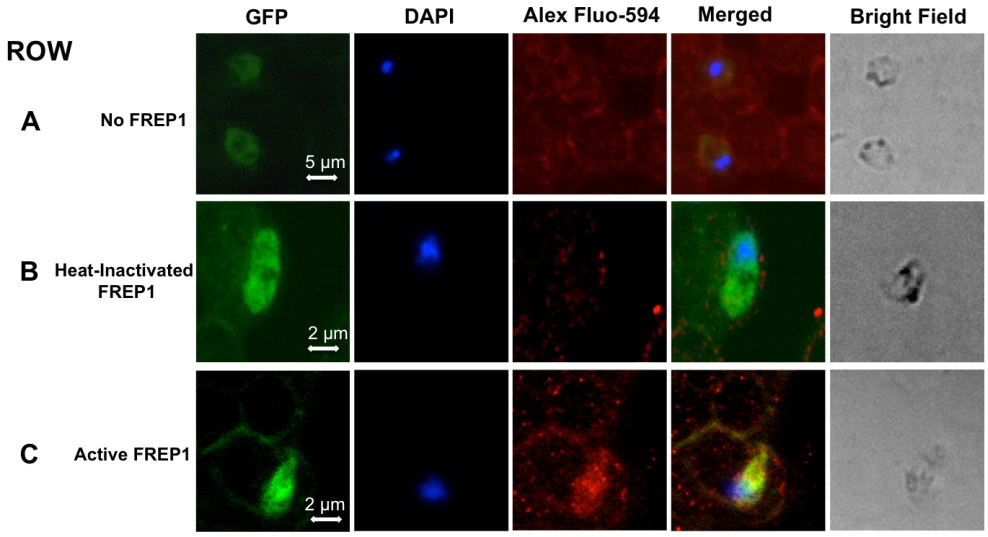

Figure 3-2. Interaction between the recombinant FREP1 and *P. berghei* demonstrated by immunofluorescence assays.
Images in rows B and C depict sexual stage parasites incubated with heat-inactivated FREP1 and active recombinant FREP1, respectively. Images in row A were obtained using the same procedures as rows B–C except no recombinant FREP1 was added. The first (GFP) and second (DAPI) columns depict parasites and nuclei staining, respectively; and the third column (Alex Fluo-594) shows FREP1 locations. Merging the first, second and third columns generate the fourth column. The last column shows cells under bright field. Scale bars were added onto the first column panels to be used for each row.

3.3.2 FREP1 was Covalently Coupled onto NHS-activated Magnetic Supports

Insect cell-expressed FREP1 was secreted into the culture medium. The purity of Ni-NTA purified FREP1 was verified using 12% SDS-PAGE gels, which demonstrated an ~95% purity level (Fig. 3-3A). Through interacting with primary amines on the FREP1 surface, N-hydroxysuccinimide (NHS) ester-activated magnetic beads were covalently coupled to FREP1 (Fig. 3-3B). The assessment of coupling efficiency was calculated from FREP1 concentration differences before and after the coupling process. As shown by SDS-PAGE, FREP1 was depleted after coupling, as indicated on silver staining SDS-PAGE (Fig. 3-3C). The calculated coupling efficiency was determined to be ~13 µg of FREP1 protein bound to one milligram of the beads,

consistent with the manufacturer's published coupling capacity and at a level of acceptable for the downstream pull-down assays.

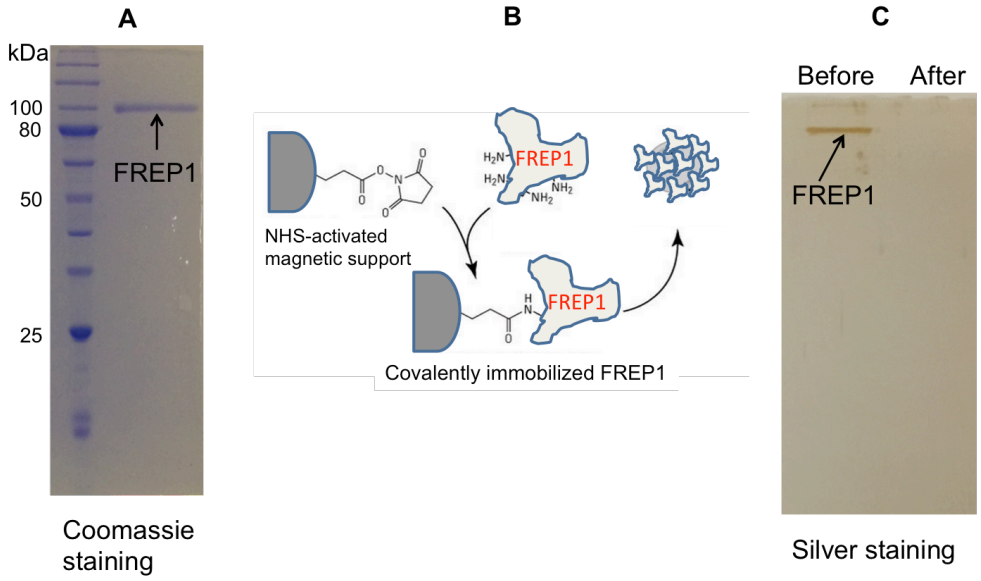

Figure 3-3. FREP1 was covalently coupled onto a magnetic support.
A, Purified recombinant FREP1 was checked on 12% SDS-PAGE gel and stained with coomassie brilliant blue. **B**, Diagram showing mechanism for FREP1 covalent immobilization onto a magnetic support. **C**, FREP1 protein levels within the supernatant examined on 12% SDS-PAGE gel. Annotations "Before" and "After" represent supernatant before and after coupling, respectively.

3.3.3 Specific Proteins Were Pulled Down and Identified Using MS

In a pull-down assay, FREP1-coupled magnetic beads were incubated with *P. berghei* infected mouse blood lysate an experiment. Glycine-coupled magnetic beads were incubated with *P. berghei* infected mouse blood lysate as a negative control. The resulting silver-stained SDS-PAGE gel clearly shows multiple specific protein bands, ranging from 15 kDa to 60 kDa, in the experimental group (*P. berghei* infected blood cell lysate) when compared with the control group (highlighted with rectangles in Fig. 3-4A).

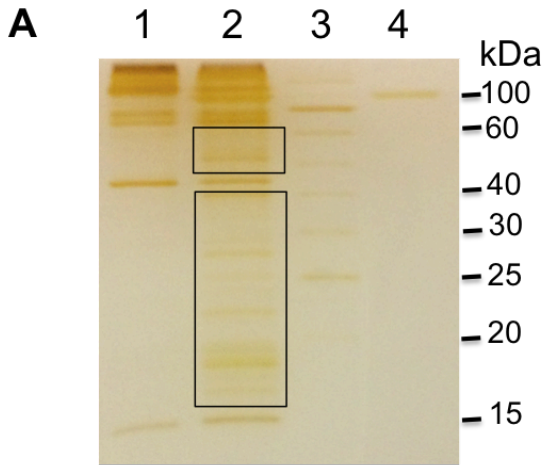

B

Accession Number	Predicted Protein Function	PEXEL Motif	Trans-Membrane Domain	MW (kDa)
PBANKA_1365500	Unknown function	+	+	37
PBANKA_0701600	Conserved *Plasmodium* protein, unknown function	-	-	26
PBANKA_0417700	Alpha tubulin 1	+	-	50
PBANKA_1316400	U1 snRNA associated protein (putative)	+	-	38
PBANKA_1309700	ATP-dependent RNA helicase DDX5 (putative)	+	-	59
PBANKA_0711900	Heat shock protein 70 (HSP70)	-	-	75
PBANKA_0307800	Conserved *Plasmodium* protein, unknown function	-	-	32
PBANKA_1133300	Elongation factor 1-alpha (EF-1alpha)	+	-	49
PBANKA_1234500	Conserved *Plasmodium* protein, unknown function	-	-	23

Figure 3-4. Pull-down of *P. berghei* iRBC lysate using FREP1 immobilized magnetic support and mass spectrometry identification result.
A, Proteins resolved on 12% SDS-PAGE following by silver staining. Areas highlighted with rectangles were enriched with specific protein bands only showing up in the experimental group. Lanes 1: *P. berghei* iRBC lysate without FREP1 immobilized NHS-ester activated beads, used as negative control; 2: *P. berghei* iRBC lysate pulled down with FREP1 immobilized NHS-ester activated beads; 3: Protein standard; 4: Purified FREP1. **B**, Mass spectrometry identification results in the experimental group after comparing with the control. "Accession Number" is consistent with the annotation on PlasmoDB *P. berghei* ANKA strain. And "+" represents "has this feature", "-" represents "no such a feature".

The protein bands from 15-60 kDa for both the control and experimental groups in Figure 3-4A were excised and analyzed, and a quantitative mass spectrometry approach was used to identify peptides within both groups. The peptides identified in these analyses were queried against the *P. berghei* (ANKA strain) protein database

(downloaded from PlasmoDB, http://plasmodb.org) and a list of protein "hits" was generated. After extensive comparison of these "hits" with the control group, and combining this with the protein identification confidence scores, nine specific FBPs were identified in the experimental group (Fig. 3-4B).

Five of these FBPs contain either a PEXEL motif or trans-membrane (TM) domains, indicating they are potential surface proteins, consistent with our indirect immunofluorescence assay (IFA) demonstrating that FREP1 interacts with surface molecules of *P. berghei* parasites. Out of the nine identified proteins, four of them have unknown functions and the remaining five are annotated with putative functions based on predictions. One of these annotations indicates a tubulin protein, PBANKA_0417700. This seems highly relevant as previously researchers have observed the *Plasmodium* ookinete ultrastructure has microtubules extended through the apical polar ring towards the extracellular space [89, 93]. This implies that tubulin proteins may potentially interact with FREP1 at the apical end, strongly supporting our proposed FREP1 working model in Chapter 2.

3.3.4 Insect Cell-expressed FBPs Interact with FREP1

The nine genes were cloned into bacmids, transfected into Sf9 cells, and expressed in High Five cells. After the third passage, cells were analyzed for FBP expression levels and the ELISA assay was performed to validate the interactions between FREP1 and recombinant FBPs. Surprisingly, all nine expressed FBPs bind FREP1 with varying binding affinities (Fig. 3-5A) after normalization, with FBP #3 being the strongest FREP1-binding factor. To further validate that the observed signals result from FBP-FREP1 interactions; an ELISA-format protein binding competition

assay was conducted. The results demonstrated that six FBPs could reduce the binding signals with FREP1 significantly (≥ 2 fold) when the FBP-FREP1 mixture was incubated in the plate, as compared to FREP1 alone (Fig. 3-5B). The remaining three FBPs had low expression levels (#5, #7, and #8) and did not show significant competition; the main reason is likely attributed to the small amount of protein present.

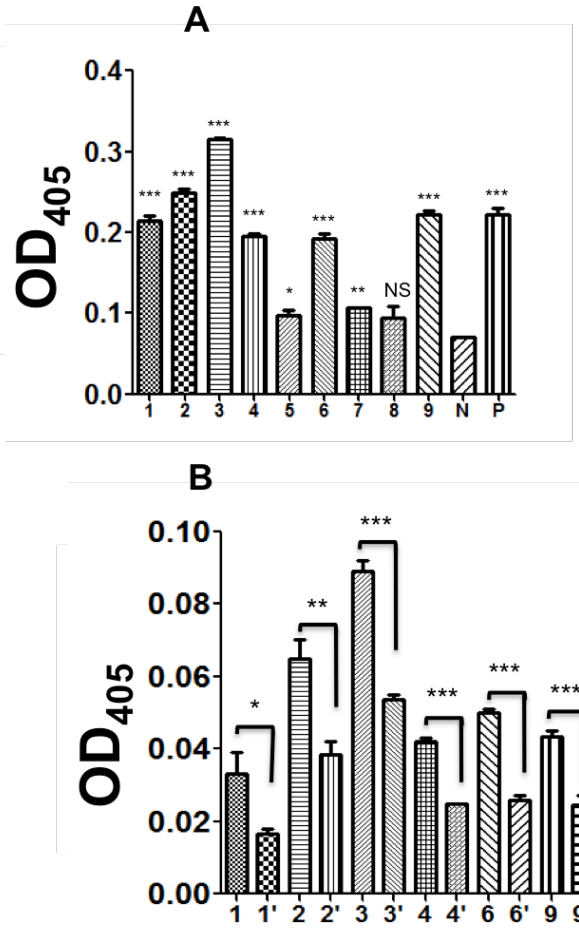

#	PlasmoDB Gene ID
1	PBANKA_1365500
2	PBANKA_0701600
3	PBANKA_0417700
4	PBANKA_1316400
5	PBANKA_1309700
6	PBANKA_0711900
7	PBANKA_0307800
8	PBANKA_1133300
9	PBANKA_1234500

Figure 3-5. Validation of the interactions between FBP candidates and FREP1.
A, ELISA approach to detect the interactions between insect cell expressed FBPs and FREP1. Negative control was performed using an irrelevant protein (CAT) expressed from the same insect cell line, and positive control was added using *P. berghei* infected RBC lysate. The correspondence of the numbers with the genes was shown in the right table, "N" represents negative control and "P" represents positive control. **B**, Protein binding competition assay was conducted using ELISA approach. Six highly expressed FBPs were coated onto a 96-well plate, and incubated with either FREP1 or FREP1/FBPs mixture (1:1 molar ratio). The gene and number correspondence are identical to panel A, with 1' represents the inhibition group for gene 1 and same

depictions for the rest genes/treatments. For both panel A and B, three replicates were performed. *p<0.05, **p<0.01,***p<0.001, NS: Not Significant; Student's *t* test.

3.3.5 FBPs Were Purified in *E. coli* and Used to Raise Antibodies in Mouse

Next, we examined whether anti-FBPs could block *Plasmodium* transmission to mice. Seven out of the nine FBPs were successfully expressed and purified from *E. coli*; the protein purities and sizes were verified on SDS-PAGE gels (Fig. 3-6A). The undetectable expression of the remaining two FBPs may be caused by the incompatibility of the expression system (like codon bias and usage). Based on the protein purification results, five of these 7 proteins were highly expressed (#2, #3, #6, #7, #8). Although two FBPs (#5 and #9) had lower expression, with a large-scale culture volume sufficient proteins (>20ug) were obtained for immunizing mice. After two boosts, day 50 sera were collected. Antibody titers were measured with an ELISA approach (Fig. 3-6B). Results show that FBP #3, #5-#8 have high immunogenicity with FBP #3 antibody titer reaching 6×10^6. Although FBP #2 has the best protein yield, it has the lowest antibody titer, indicating this protein is low immunogenic.

Further experiments of examining antibodies in blocking *Plasmodium* transmission is ongoing.

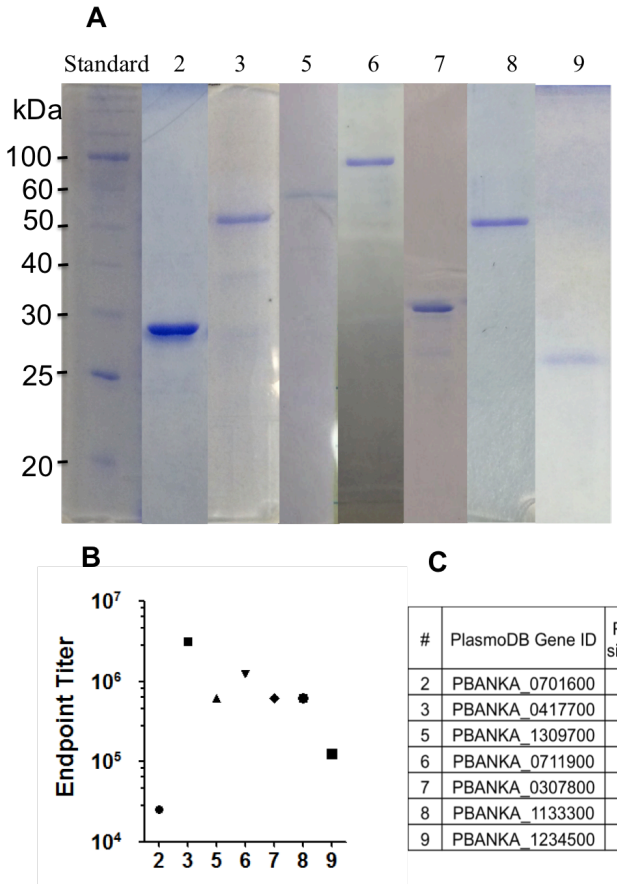

#	PlasmoDB Gene ID	Protein size/kDa
2	PBANKA_0701600	27.3
3	PBANKA_0417700	52.3
5	PBANKA_1309700	62.6
6	PBANKA_0711900	76.6
7	PBANKA_0307800	33.5
8	PBANKA_1133300	50.4
9	PBANKA_1234500	24.9

Figure 3-6. Purification of FBP proteins from *E. coli* and anti-FBP antibodies production in mice.
A, The purification of seven FBPs after being over-expressed in *E. coli* were checked using 12% SDS-PAGE gel, and the calculated protein sizes that correspond with the gene IDs are shown in panel **C**. **B**, Anti-FBP antibodies were raised in mouse and antibody endpoint titer (day 50) was checked using ELISA approach after two boosts. X-axis coordinates correspond with the gene IDs within panel **C**.

3.4 Discussion

Mosquito midgut peritrophic matrix FREP1 was discovered to facilitate *P. falciparum* infection in *An. gambiae* mosquitoes through binding to *P. falciparum* ookinetes [11, 12]. We hypothesized that *P. falciparum* ookinete surface molecules should be involved in binding with mosquito FREP1. This chapter demonstrate that *P. berghei* parasites also bind FREP1, highlighting the conservation of this invasion

mechanism. Moreover, we tried to identify the FREP1 binding partner(s) from *P. berghei* using a pull-down approach followed by identification using mass spectrometry analysis. Mass spectrometry comparative analysis identified nine candidate FBPs from pull-down assays. We cloned and expressed these FBPs in insect cells. Surprisingly, all of the nine recombinant FBP proteins interacted with FREP1 in ELISA assays, although the apparent strength of interaction did vary. While it is difficult to imagine that all nine FBP proteins characterized by pull-down interact with FREP1, it is possible that FREP1 binds to a common motif among all FBPs, such as a lipid or a carbohydrate post-translational modification. Continued study will be needed to understand the molecular mechanism of FREP1-mediated *Plasmodium* invasion pathways.

Plasmodium surface molecules have been recognized as promising anti-malarial targets. Research has focused on the merozoite stage surface proteins for decades [94-98]. However, malaria vaccines or anti-malarial drugs targeting these antigens had poor outcomes in clinical trials due to their low immunogenicity and protection from red blood cell membrane [50]. In contrast, malaria transmission blocking vaccines (TBV) have shown more promising results because these take advantage of the malaria transmission bottleneck in the mosquito midgut. Furthermore, molecules from both of the sexual-stage malaria parasites and the mosquito midguts can act as candidate targets for developing TBVs. A mosquito midgut protein, FREP1, has been discovered and characterized as one of the best TBV candidates [12]. From this study, we have identified nine FREP1 binding partners from *P. berghei* parasites. More efficient anti-malarial strategies could be developed if both FREP1 and FBPs were targeted with combination therapies.

Chapter 4 : Interactome of Mosquito Midgut and *Plasmodium* Parasites

4.1 Introduction

Mosquito species are an essential vector for malaria transmission, and *Plasmodium* parasites have to survive in the hostile environment of the mosquito midgut to progress to infection [5]. Previously, mosquito midgut proteins were found to be essential for parasite infection of the mosquito midgut [11, 12, 20, 23, 33]. In addition, some *Plasmodium* ookinete proteins, including CTRP, SOAP, CelTOS, PPLP-4/5, have been discovered to be important or even indispensable for parasite infection in the mosquito midgut [24, 25, 28-30]. Protein-interactions between *Plasmodium* parasites and the mosquito midgut have critical roles for successful *Plasmodium* transmission to mosquitoes.

Despite many decades of research, the molecular mechanisms of *Plasmodium* invasion in mosquito midgut remain largely unknown. In recent years, high-throughput scientific methods have been developed to rapidly optimize the study of large numbers of molecules; for instance, DNA microarray techniques have been widely applied to identify transcription factor binding sites or to detect gene mutations and deletions in genome-wide research [99, 100]. Similarly, with the increasing development of proteomics, large-scale investigation of proteins has become highly desired, necessitating advances in high-throughput protein interaction techniques. The first "proteome library" and its use in protein microarray were achieved in yeast by Heng Zhu and colleagues [101]. Continual improvements in the protein microarray technique

have facilitated studies of protein-protein interactions [102], protein-DNA interactions [103], protein-receptor interactions [104] and antigen-antibody interactions [105].

In this chapter, the goal was to identify additional mosquito midgut proteins that interact *Plasmodium falciparum* by 1) establishing a computational database that contains *An. gambiae* midgut secretory proteins; 2) expressing selected identified mosquito midgut proteins in insect cells; and 3) identifying mosquito midgut proteins that interact with *Plasmodium falciparum*.

4.2 Experimental Materials and Methods

4.2.1 Computational Approach to Predict *An. gambiae* Mosquito Midgut Proteins that Potentially Interact with *P. falciparum* Parasites

A *An. gambiae* secretory midgut protein database ("secretome") was established based mainly on three criteria: a) the presence of a signal peptide or transmembrane domain(s) based on the bioinformatic resource VectorBase [106]; b) up-regulation by a blood meal; and c) preferential expression in the midgut, with the latter two criteria based on published RNA microarray data [107]. Either signal peptide or transmembrane domains should present within the candidate proteins because we are seeking secretory proteins in the mosquito midgut. Blood meals affect mosquito gene expressions [108], some of which are involved in *Plasmodium* invasion. These upregulated genes may be used as a means of mosquito defence and parasites may take advantage of these molecules for their invasion. Some of these up-regulated gene products are responsible for digesting blood in the mosquito midgut lumen [109]. We have focused on gene up-regulation happening 12-24 h after a blood meal because this correlates with ookinete

maturation and invasion. Using the above criteria, we created a comprehensive set of candidate *Anopheles* genes for further analysis.

4.2.2 Expression of Recombinant Proteins in Insect Cells.

PCR oligos were designed (see Table 4-1) to amplify candidate genes from the cDNA library of *An. gambiae* adult female mosquitoes. PCR products were digested with restriction enzymes, and ligated into pFastBac1 plasmid (a 6×His tag was added to the C-terminus of each expressed protein); recombinant plasmids were transformed into *E. coli* DH10Bac competent cells. Blue-white colony selection was used for recombinant bacmid verification, and isolated bacmids were used to transfect an Sf9 insect cell line. For high secretory protein yield, a High Five insect cell line was used for downstream infection. Protein expression was confirmed with an ELISA approach based on recognition of the engineered 6×His-tag by a monoclonal anti-His antibody.

Table 4-1. PCR primers of 15 *An. gambiae* midgut genes.

Gene ID	Primer Name	Primer Sequence
AGAP003573-PA	Forward	5'-CGGAATTCGCCCAAAGCTTTAAAATGCGTATCCT-3'
	Reverse	5'-GCTCTAGAGTTGGTAAGCATTTTCTTCAG-3'
AGAP006972-PA	Forward	5'-CGGAATTCATGTTTAAGTTCGTTGCCGTG-3'
	Reverse	5'-GCTCTAGATCCGTGATGGTGATGGTGGTG-3'
AGAP008463-PA	Forward	5'-CGGAATTCATGAAGGGATTCATCGCGATCG-3'
	Reverse	5'-GCTCTAGACGCCACAATCGACTTCTGGTTG-3'
AGAP001508-PA	Forward	5'-CGGAATTCATGAAGTCCTTCTCGTGTCTG-3'
	Reverse	5'-GCTCTAGATCCTCCGAACGACTGGGCAC-3'
AGAP011006-PA	Forward	5'-CGGAATTCGTAGCACAGATCACGATGAACG-3'
	Reverse	5'-GCTCTAGAATCGTCAATTGGTACTCTTTTCAGC-3'
AGAP008138-PA	Forward	5'-CGGAATTCATGCTGCTAAAATCGGCACTAC-3'
	Reverse	5'-GCTCTAGAAACAGCCACCGGTCCGGTGAG-3'
AGAP006425-PA	Forward	5'-CGGAATTCTTAGCAAGATGAGACGAATCG-3'
	Reverse	5'-GCTCTAGAATGATCTCCCGGAATCAACAC-3'
AGAP00	Forward	5'-CGGAATTCACCACAACCATGTACAAGTTC-3'

1956-PA	Reverse	5’-GCTCTAGAACCGACGATCGCTGCATCGATTTC-3’
AGAP00	Forward	5’-CGGAATTCGCAAGGATTGCAAGATGTTC-3’
2848-PA	Reverse	5’-GCTCTAGACAGCAGCGTCACGGT-3’
AGAP00	Forward	5’-CGGAATTCAAACGTGATGAAATCTC-3’
1240-PA	Reverse	5’-GCTCTAGAGGCTAGCCATTTCTTTACCAG-3’
AGAP00	Forward	5’-CGGGATCCATGGCACGGAGAACAACACAC-3’
3629-PA	Reverse	5’-CGGAATTCCTAGTAGTTGCCGTGACAGCAGTGTG-3’
AGAP00	Forward	5’-CGGGATCCATGCGTATAGTCATGTTGTG-3’
3926-PA	Reverse	5’-GCTCTAGATTGGTGCCCTTCCCGCTCGTAAATG-3’
AGAP00	Forward	5’-CGGAATTCATGCAGCTCCTAGTGGCAGTGTTG-3’
2851-PA	Reverse	5’-GCTCTAGAGACTACTTTCGCTTCCAGCTG-3’
AGAP00	Forward	5’-CGGGATCCATGTTTAAAACGTGTTTAGGGATTG-3’
4918-PA	Reverse	5’-CGGAATTCCAGCTCGCAGCCATTTGGGCCTTAT-3’
AGAP00	Forward	5’-CGGAATTCGCTACAACTTTTAGAAATGAA-3’
1193-PA	Reverse	5’-GCTCTAGACGTGCGAAAAATTAGACCAAC-3’

Note: The underlined sequences are restriction recognition sites.

4.2.3 ELISA and IFA approaches to Verify Protein-Parasite Interactions

Similar to the ELISA protocol in Chapter 3, day 15 *in vitro* cultured *P. falciparum* gametocytes were harvested and lysed in cell lysis buffer, and the protein concentration in the lysate was measured using the Bradford method [110]. *P. falciparum* parasite protein mixture (50 µL at 3 µg/mL) was coated onto clear 96-well plates overnight at 4°C; the plate was blocked with 1 % BSA for 2 h at room temperature (RT), and then washed three times with 1×PBS containing 0.05% (v/v) Tween-20 (PBST). Expressed recombinant proteins (500 ng) were added into wells to react with the coated lysate: an equivalent amount of CAT protein (Chloramphenicol acetyltransferase with a C-terminal 6×His-tag) was included as negative control. After 1 h incubation, three washes were performed with PBST before incubating with 1:1,000 diluted anti-His monoclonal antibody (LifeTein, LLC, New Jersey, USA) for 1 h, washed with PBST and followed by a 1:10,000 diluted goat anti-mouse IgG (conjugated

with alkaline phosphatase) for 1 h. Plates were developed with *p*-nitrophenylphosphate (*p*NPP) for 30 min. and the absorbance was measured at 405 nm.

For indirect immunofluorescence assay (IFA), day 15 *in vitro* cultured *P. falciparum* gametocytes were harvested and coated onto glass coverslips and then sequentially: 1) fixed with 4 % paraformaldehyde for 30 min, 2) quenched with 100 mM glycine in 1×PBS for 20 min, 3) washed three times with 1×PBS, 4) blocked with 1 % BSA overnight at 4°C. The next day, the coverslip was incubated with 100 mg expressed candidate protein for 2 h, and probed for 1 h with 1:1,000 diluted anti-His monoclonal antibody (LifeTein, LLC, New Jersey,USA). After washing three times with 1×PBS, bound protein signals were further amplified by incubating with 1:10,000 diluted Alexa Fluor 555 Goat Anti-Mouse antibody (Invitrogen, Carlsbad, USA) for 30 min. Then, the coverslips were air-dried for 30 min after being washed three times with 1×PBS. A small drop of mounting medium containing 4', 6-Diamidino-2-Phenylindole (DAPI) (Vector laboratories, Inc. Burlingame, CA) was placed onto glass slides, and coverslips were mounted on top of the slides. Finally, the results were visualized using a Nikon Eclipse Ti-S fluorescent microscope.

4.2.4 *in vitro* Synthesis of dsRNA and SMFA

Oligomers were designed for RNA interference of the candidate genes using the E-RNAi web server, ensuring they contained a T7 promoter sequence (Horn, 2010) (Table 4-2). Double stranded RNAs (dsRNA) were synthesized with the MEGAscript Kit (Life Technology). One-day-old adult female mosquitoes were used for dsRNA microinjection, wherein ~67 nL of 3 μg/μL of dsRNA was injected into the thorax of each adult mosquito using a Nanoject II micro-injector (Drummond Scientific

Company). Approximately 100 female mosquitoes were injected for each candidate gene, and an equivalent amount of GFP dsRNA was injected into mosquitoes as a negative control.

Table 4-2. Primer table for dsRNA synthesis

Gene ID	Primer Name	Primer Sequence
5070	RNAi-Forward	TAATACGACTCACTATAGGGGGCGGTAGTAGTTACAGCACG
	RNAi-Reverse	TAATACGACTCACTATAGGGGTCAGCGGACAGGAAGTGTT
9641	RNAi-Forward	TAATACGACTCACTATAGGGATCGTTCGATCTGGTCGATAA
	RNAi-Reverse	TAATACGACTCACTATAGGGAGGGTCAACCGATCGAGAAT
2367	RNAi-Forward	TAATACGACTCACTATAGGGGTGCAGATTCGCTTCCTTTC
	RNAi-Reverse	TAATACGACTCACTATAGGGGACTGTCCTGGGACTCTTGG
5073	RNAi-Forward	TAATACGACTCACTATAGGGCCATTCCGTACCATCACATTC
	RNAi-Reverse	TAATACGACTCACTATAGGGCACATGCCCCCTACAAGC

Note: The underlined sequences are T7 promoter.

Treated mosquitoes were fed at 48 h post-injection with 0.2 % *P. falciparum* gametocytes (day 15 *in vitro* cultured) using a standard membrane feeding assay (SMFA) [78]; engorged mosquitoes were maintained at 27°C and 80% humidity with 10% sugar for 7 days. Mosquito midguts were then dissected and stained with 0.1% mercury dibromofluorescein disodium salt in 1×PBS, and the number of oocysts in each midgut was counted using a light microscope.

4.3 Results

4.3.1 Compilation of *An. gambiae* Midgut Secretory Proteins

Ninety five genes were predicted as candidates for interactions between a *An. gambiae* midgut and a *Plasmodium* parasite (see Appendix Table). Distribution of the

predicted candidate genes shows high variability with respect to their presumed functions (Fig. 4-1). Of these candidates, 21% of the genes have predicted protease activity, which correlates closely with the increased digestion demands in the mosquito midgut lumen after a blood meal. Among the other identified candidates, 12% of the genes have predicted defense functions, and 5% have lipid/chitin binding functions. These two groupings are interesting candidates for further functional studies because they are likely to be involved in parasite-mosquito interactions. The remaining 36% of the compiled genes' functions are unknown. It is worth noting that the FREP1 is among predicted candidate genes.

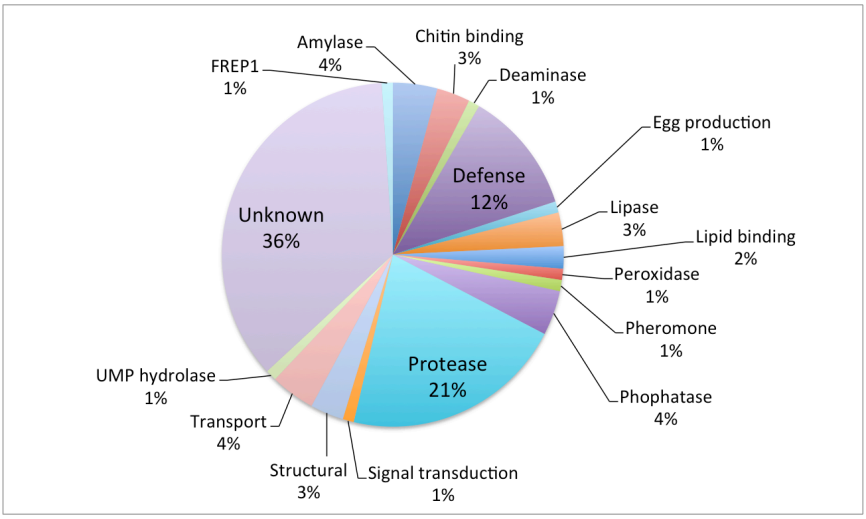

Figure 4-1. Predicted functions for candidate *An. gambiae* midgut secretome.
95 mosquito midgut proteins are candidates and the corresponding percentage for each category is indicated relative to the total.

4.3.2 Four Expressed Proteins Were Found Interacting with *P. falciparum* by Both ELISA and IFA

Out of the 95 genes, 15 genes were chosen arbitrarily, mainly from the defense or lipid/chitin binding predicted functions, for further study. The 15 proteins were

expressed in High Five cells based on ELISA utilizing the anti-His antibody because all of the recombinant proteins have 6×His tag at the protein C-termini. Notably, 10 out of these 15 proteins show significant interacting signals with *P. falciparum* parasite lysate through ELISA compared with negative control (Fig. 4-2). To assess if these interacting molecules come from the parasite cell membrane, a non-permeabilized IFA approach was used. *P. falciparum* parasites were fixed on glass slides and monitored for interactions with ten candidate proteins. Four of them showed co-localization with the parasites (Fig. 4-3), supporting them on *P. falciparum* infected cell surface, which will be further analyzed.

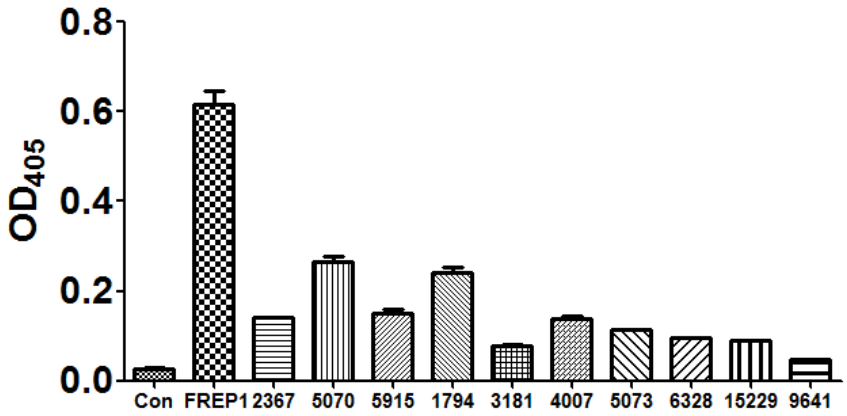

Figure 4-2. ELISA verification of the interactions between 10 candidate genes and *P. falciparum* infected cell lysate.
X-axis represents the name of candidate genes (using gene ID from omics.fiu.edu), whose correspondence with vectorbase gene ID can be found in the Appendix Table. Y-axis shows the absorbance value under 405 nm with subtraction of the absorbance under 405 nm. Using Student's *t* test, all ten genes show significant ($p<0.01$) higher interacting signals than the negative control ("Con").

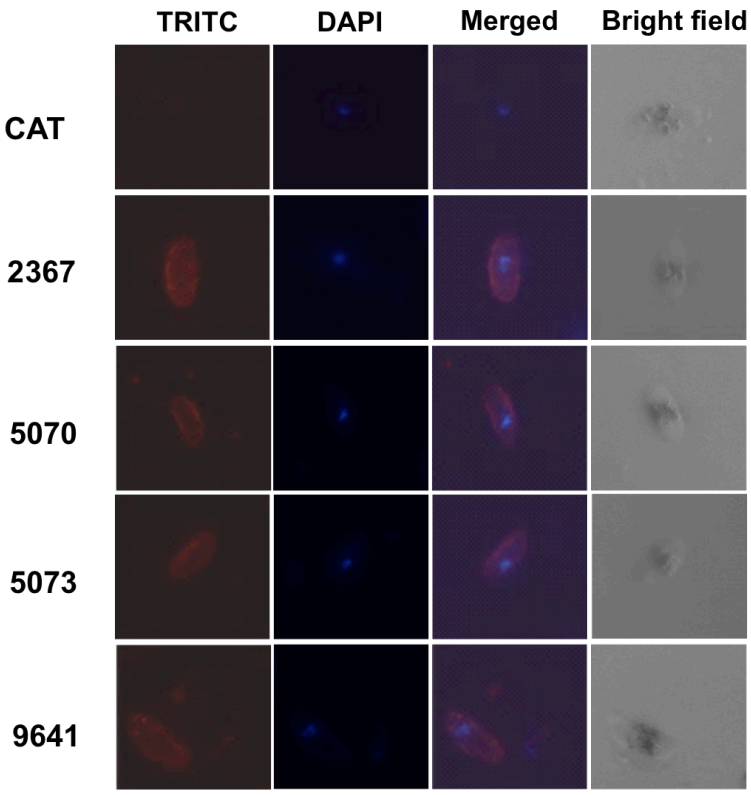

Figure 4-3. IFA experiments of four proteins that interact with *P. falciparum* surface molecules.
4% paraformaldehyde-fixed *P. falciparum* gametocytes were incubated with candidate proteins and negative control (CAT). The first (TRITC) and second columns (DAPI) depict candidate protein locations and parasite nuclear staining, respectively. Merging the first, second columns generated the third column. The last column shows parasites under the bright field.

4.3.3 Assessing Candidate Gene Function in Parasite Invasion using RNAi

From the identification results in section 4.3.2, four genes were further analyzed using RNA interference for their functional roles in malaria infection. Double-stranded RNA for each of the four candidate genes was injected into female mosquitoes, and a CAT gene was used as the negative control. Seven days later, mosquito midguts were dissected and oocyst numbers per midgut were compared with the control. The normal function of gene *2367* and *5070* was likely to be inhibitory of *P. falciparum* infection, indicated by a significant ($p<0.01$) increase of the oocyst infection in the mosquito

midgut after gene knockdown as compared to the control group (Fig. 4-4C and D). In contrast, the other two genes, *5073* and *9641*, showed completely opposite results, suggesting that the normal function of these two genes is to facilitate *Plasmodium* infection (Fig. 4-4A and B). Accordingly, this indicates that mosquito genes can be involved in parasite infection through either facilitating or inhibiting invasion. This is consistent with our previous observation that despite being from the same family, the FBN30 and FREP1 proteins have opposite effects during malaria parasite infection of mosquitoes [11]. In summary, the four *Plasmodium*–interacting mosquito midgut proteins we have identified can either promote or inhibit malaria parasite infection in mosquitoes: however, the detailed molecular mechanisms remain unknown.

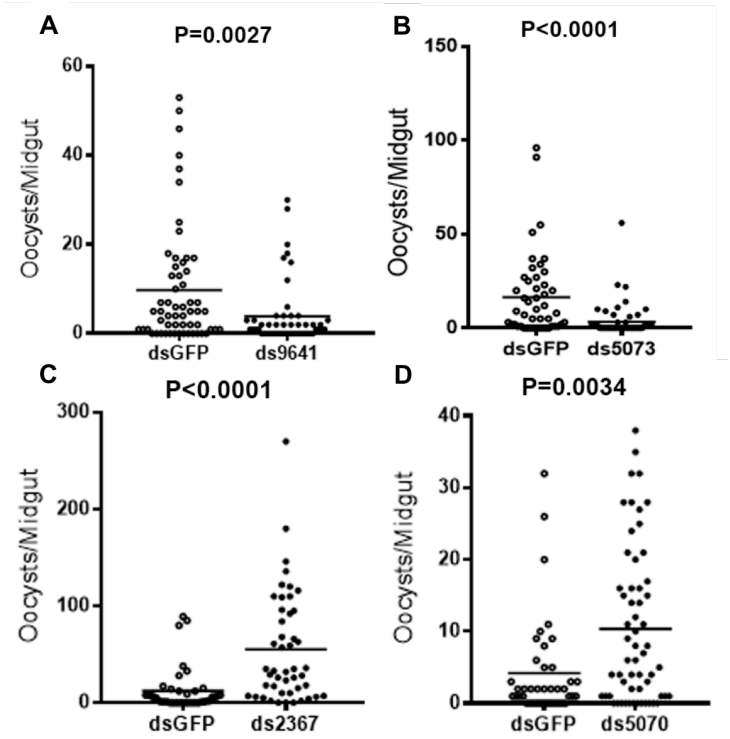

Figure 4-4**. RNAi experiments demonstrate the effects on *P. falciparum* infection after candidate gene knockdown.**
Data summary and statistical analyses of the oocyst numbers in mosquitoes treated with either GFP dsRNA or candidate gene dsRNA (Panel A-D). Y-axis represents the

number of oocyst per midgut and x-axis indicates treatment groups. The black bars represent the mean of oocyst numbers per midgut, and p values between two groups were calculated using Wilcoxon-Mann-Whitney test. Data are consistent with two independent experiments.

4.4 Discussion

A mosquito midgut secretory protein database, potentially useful for examining *Plasmodium* infection mechanisms in the mosquito midgut, was generated using computational approaches. These approaches resulted in approximately one hundred midgut proteins after screening the *An. gambiae* genome that contains ~13,000 coding genes. In our study, computational approaches narrowed down the gene pool of interest dramatically and improved the working efficiency by two orders of magnitude.

Experimental validation of candidate protein interaction by ELISA and IFA identified 4 mosquito midgut proteins that may interact with the *P. falciparum* cell surface (Fig. 4-3). RNA interference showed two genes (*5073* and *9641*) facilitated *P. falciparum* infection while other two (*2367* and *5070*) inhibited *P. falciparum* infection.

Two mosquito midgut genes, *2367* and *5070*, served to inhibit *P. falciparum* infection in mosquitoes; they have been putatively annotated as keratin associated protein (KRTAP) and epididymal secretory protein E1, respectively. Epididymal secretory protein E1 controls sterol homeostasis and steroid biosynthesis in *Drosophila* [111], however, it is not established whether it is needed for mosquito species. Unlike most animals, insects lack the capacity to synthesize sterols, which are essential in lipid bio-structures and are required as precursors of important steroid hormones; therefore insects must acquire sterols from their diet [112]. In our study, the results (Fig. 4-4D) lead us to speculate that it might be easier for malaria parasites to infect mosquitoes after the sterol hemostasis disruption as we hypothesize that the sterol homeostasis and

steroid biosynthesis of mosquitoes might be affected once the expression of the Epididymal secretory protein E1 gene was reduced. Keratin associated proteins (KRTAPs) are one of the major components of hair-like structures and play essential roles in the formation of rigid and resistant hair shafts [113]. However, little research has been done on their functions in insects. In our study, the results (Fig. 4-4C) revealed that the knockdown of keratin-associated protein gene expression increases *P. falciparum* parasites infection, suggesting that this protein family may not only be a component of mammalian hair, but also be endowed with some malaria infection-relevant roles in mosquitoes.

In contrast, the other two mosquito midgut genes, *5073* and *9641*, were identified to facilitate *P. falciparum* infection in mosquitoes. Gene *5073* was annotated as a Niemann-Pick C2 (NPC2) protein in our protein database. It is generally known that cholesterol is an important precursor for numerous biologically active molecules, and it plays a major role in membrane structures and functions. NPC2 protein has been characterized as a cholesterol-binding and -transport protein, whose function loss typically leads to NPC2 disease (an inherited neurodegenerative disorder) [114, 115]. In this study, the mean number of *P. falciparuam* oocysts per midgut was significantly reduced in gene knockdown mosquitoes than that in control, implying that *Plasmodium* infection might need the homeostasis of cholesterol. Gene *9641* was predicted as 3-phosphoshikimate 1-carboxyvinyltransferase (also known as 5-enolpyruvylshikimate-3-phosphate synthase, EPSP), which is an enzyme in biosynthesis of aromatic amino acids in plants, many bacteria, and microbes, and also a prime target for drugs and herbicides [116]. Our results indicated that *P. falciparuam* oocyst numbers per midgut were

significantly reduced when gene *9641* was silenced in mosquitoes (Fig. 4-4A). Since malaria parasites have limited capabilities to biosynthesize amino acids [117], we speculate that the knockdown of gene *9641* might damage the biosynthesis of aromatic amino acids in *Anopheline* mosquitoes, and as a consequence, the *Plasmodium* infection in mosquito midguts was impaired because of a lack of sufficient aromatic amino acids for parasite development.

In summary, we developed a computational approach and identified 95 mosquito midgut secretory proteins that may potentially interact with *Plasmodium* and affect its ability to effectively invade and develop in mosquitoes. Based on the experimental results, 4 (out of fifteen) proteins were identified to interact with *Plasmodium* surface molecules and play either facilitating or inhibitory roles for parasite propagation in the mosquito midgut. Following a similar approach, more mosquito midgut proteins that are implicated in malaria transmission may be discovered, precipitating a more comprehensive understanding of the molecular mechanisms of malaria transmission.

References

1. Phillips, R.S., *Current status of malaria and potential for control.* Clin Microbiol Rev, 2001. **14**(1): p. 208-26.

2. Ogwan'g, R.A., et al., *Factors affecting exflagellation of in vitro-cultivated Plasmodium falciparum gametocytes.* Am J Trop Med Hyg, 1993. **49**(1): p. 25-9.

3. Bongfen, S.E., et al., *Genetic and genomic analyses of host-pathogen interactions in malaria.* Trends Parasitol, 2009. **25**(9): p. 417-22.

4. Baton, L.A. and L.C. Ranford-Cartwright, *How do malaria ookinetes cross the mosquito midgut wall?* Trends Parasitol, 2005. **21**(1): p. 22-8.

5. Linser, P.J., et al., *Carbonic anhydrases and anion transport in mosquito midgut pH regulation.* J Exp Biol, 2009. **212**(Pt 11): p. 1662-71.

6. Abraham, E.G. and M. Jacobs-Lorena, *Mosquito midgut barriers to malaria parasite development.* Insect Biochem Mol Biol, 2004. **34**(7): p. 667-71.

7. Sinden, R.E., *The cell biology of malaria infection of mosquito: advances and opportunities.* Cell Microbiol, 2015. **17**(4): p. 451-66.

8. Ghosh, A.K., et al., *Plasmodium ookinetes coopt mammalian plasminogen to invade the mosquito midgut.* Proc Natl Acad Sci U S A, 2011. **108**(41): p. 17153-8.

9. Huber, M., E. Cabib, and L.H. Miller, *Malaria parasite chitinase and penetration of the mosquito peritrophic membrane.* Proc Natl Acad Sci U S A, 1991. **88**(7): p. 2807-10.

10. Vinetz, J.M., et al., *Chitinases of the avian malaria parasite Plasmodium gallinaceum, a class of enzymes necessary for parasite invasion of the mosquito midgut.* J Biol Chem, 2000. **275**(14): p. 10331-41.

11. Li, J., et al., *Genome-block expression-assisted association studies discover malaria resistance genes in Anopheles gambiae.* Proc Natl Acad Sci U S A, 2013. **110**(51): p. 20675-80.

12. Zhang, G., et al., *Anopheles Midgut FREP1 Mediates Plasmodium Invasion.* J Biol Chem, 2015. **290**(27): p. 16490-501.

13. Ramasamy, M.S., et al., *Interactions of human malaria parasites, Plasmodium vivax and P.falciparum, with the midgut of Anopheles mosquitoes.* Med Vet Entomol, 1997. **11**(3): p. 290-6.

14. Shen, Z., et al., *A cell surface mucin specifically expressed in the midgut of the malaria mosquito Anopheles gambiae.* Proc Natl Acad Sci U S A, 1999. **96**(10): p. 5610-5.

15. Morlais, I. and D.W. Severson, *Identification of a polymorphic mucin-like gene expressed in the midgut of the mosquito, Aedes aegypti, using an integrated bulked segregant and differential display analysis.* Genetics, 2001. **158**(3): p. 1125-36.

16. Dinglasan, R.R., et al., *Plasmodium falciparum ookinetes require mosquito midgut chondroitin sulfate proteoglycans for cell invasion.* Proc Natl Acad Sci U S A, 2007. **104**(40): p. 15882-7.

17. Dinglasan, R.R., et al., *Disruption of Plasmodium falciparum development by antibodies against a conserved mosquito midgut antigen.* Proc Natl Acad Sci U S A, 2007. **104**(33): p. 13461-6.

18. Sinden, R.E. and P.F. Billingsley, *Plasmodium invasion of mosquito cells: hawk or dove?* Trends Parasitol, 2001. **17**(5): p. 209-12.

19. Ghosh, A.K., P.E. Ribolla, and M. Jacobs-Lorena, *Targeting Plasmodium ligands on mosquito salivary glands and midgut with a phage display peptide library.* Proc Natl Acad Sci U S A, 2001. **98**(23): p. 13278-81.

20. Zieler, H., et al., *A snake venom phospholipase A(2) blocks malaria parasite development in the mosquito midgut by inhibiting ookinete association with the midgut surface.* J Exp Biol, 2001. **204**(Pt 23): p. 4157-67.

21. Ito, J., et al., *Transgenic anopheline mosquitoes impaired in transmission of a malaria parasite.* Nature, 2002. **417**(6887): p. 452-5.

22. Moreira, L.A., et al., *Bee venom phospholipase inhibits malaria parasite development in transgenic mosquitoes.* J Biol Chem, 2002. **277**(43): p. 40839-43.

23. Rodriguez Mdel, C., et al., *The surface protein Pvs25 of Plasmodium vivax ookinetes interacts with calreticulin on the midgut apical surface of the malaria vector Anopheles albimanus.* Mol Biochem Parasitol, 2007. **153**(2): p. 167-77.

24. Dessens, J.T., et al., *CTRP is essential for mosquito infection by malaria ookinetes.* EMBO J, 1999. **18**(22): p. 6221-7.

25. Dessens, J.T., et al., *SOAP, a novel malaria ookinete protein involved in mosquito midgut invasion and oocyst development.* Mol Microbiol, 2003. **49**(2): p. 319-29.

26. Ishino, T., et al., *A calcium-dependent protein kinase regulates Plasmodium ookinete access to the midgut epithelial cell.* Mol Microbiol, 2006. **59**(4): p. 1175-84.

27. Kadota, K., et al., *Essential role of membrane-attack protein in malarial transmission to mosquito host.* Proc Natl Acad Sci U S A, 2004. **101**(46): p. 16310-5.

28. Wirth, C.C., et al., *Perforin-like protein PPLP4 is crucial for mosquito midgut infection by Plasmodium falciparum.* Mol Biochem Parasitol, 2015. **201**(2): p. 90-9.

29. Ecker, A., et al., *Plasmodium berghei: plasmodium perforin-like protein 5 is required for mosquito midgut invasion in Anopheles stephensi.* Exp Parasitol, 2007. **116**(4): p. 504-8.

30. Kariu, T., et al., *CelTOS, a novel malarial protein that mediates transmission to mosquito and vertebrate hosts.* Mol Microbiol, 2006. **59**(5): p. 1369-79.

31. Tomas, A.M., et al., *P25 and P28 proteins of the malaria ookinete surface have multiple and partially redundant functions.* EMBO J, 2001. **20**(15): p. 3975-83.

32. Kotsyfakis, M., et al., *Plasmodium berghei ookinetes bind to Anopheles gambiae and Drosophila melanogaster annexins.* Mol Microbiol, 2005. **57**(1): p. 171-9.

33. Lavazec, C., et al., *Carboxypeptidases B of Anopheles gambiae as targets for a Plasmodium falciparum transmission-blocking vaccine.* Infect Immun, 2007. **75**(4): p. 1635-42.

34. Gonzalez-Lazaro, M., et al., *Anopheles gambiae Croquemort SCRBQ2, expression profile in the mosquito and its potential interaction with the malaria parasite Plasmodium berghei.* Insect Biochem Mol Biol, 2009. **39**(5-6): p. 395-402.

35. Saraiva, R.G., et al., *Mosquito gut antiparasitic and antiviral immunity.* Dev Comp Immunol, 2016. **64**: p. 53-64.

36. Blandin, S., et al., *Complement-like protein TEP1 is a determinant of vectorial capacity in the malaria vector Anopheles gambiae.* Cell, 2004. **116**(5): p. 661-70.

37. Fraiture, M., et al., *Two mosquito LRR proteins function as complement control factors in the TEP1-mediated killing of Plasmodium.* Cell Host Microbe, 2009. **5**(3): p. 273-84.

38. Dong, Y., et al., *Anopheles gambiae immune responses to human and rodent Plasmodium parasite species.* PLoS Pathog, 2006. **2**(6): p. e52.

39. Ramphul, U.N., et al., *Plasmodium falciparum evades mosquito immunity by disrupting JNK-mediated apoptosis of invaded midgut cells.* Proc Natl Acad Sci U S A, 2015. **112**(5): p. 1273-80.

40. Garver, L.S., G. de Almeida Oliveira, and C. Barillas-Mury, *The JNK pathway is a key mediator of Anopheles gambiae antiplasmodial immunity.* PLoS Pathog, 2013. **9**(9): p. e1003622.

41. Dong, Y. and G. Dimopoulos, *Anopheles fibrinogen-related proteins provide expanded pattern recognition capacity against bacteria and malaria parasites.* J Biol Chem, 2009. **284**(15): p. 9835-44.

42. Christensen, B.M., et al., *Melanization immune responses in mosquito vectors.* Trends Parasitol, 2005. **21**(4): p. 192-9.

43. Volz, J., et al., *A genetic module regulates the melanization response of Anopheles to Plasmodium.* Cell Microbiol, 2006. **8**(9): p. 1392-405.

44. Michel, K., et al., *Anopheles gambiae SRPN2 facilitates midgut invasion by the malaria parasite Plasmodium berghei.* EMBO Rep, 2005. **6**(9): p. 891-7.

45. Abraham, E.G., et al., *An immune-responsive serpin, SRPN6, mediates mosquito defense against malaria parasites.* Proc Natl Acad Sci U S A, 2005. **102**(45): p. 16327-32.

46. Wang, S. and M. Jacobs-Lorena, *Genetic approaches to interfere with malaria transmission by vector mosquitoes.* Trends Biotechnol, 2013. **31**(3): p. 185-93.

47. Wang, J., et al., *Haem-activated promiscuous targeting of artemisinin in Plasmodium falciparum.* Nat Commun, 2015. **6**: p. 10111.

48. Noedl, H., et al., *Evidence of artemisinin-resistant malaria in western Cambodia.* N Engl J Med, 2008. **359**(24): p. 2619-20.

49. Niu, G., et al., *Targeting mosquito FREP1 with a fungal metabolite blocks malaria transmission.* Sci Rep, 2015. **5**: p. 14694.

50. Thera, M.A. and C.V. Plowe, *Vaccines for malaria: how close are we?* Annu Rev Med, 2012. **63**: p. 345-57.

51. Atkinson, S.C., et al., *The Anopheles-midgut APN1 structure reveals a new malaria transmission-blocking vaccine epitope.* Nat Struct Mol Biol, 2015. **22**(7): p. 532-9.

52. Raz, A., N. Dinparast Djadid, and S. Zakeri, *Molecular characterization of the carboxypeptidase B1 of Anopheles stephensi and its evaluation as a target for transmission-blocking vaccines.* Infect Immun, 2013. **81**(6): p. 2206-16.

53. Ghosh, A.K. and M. Jacobs-Lorena, *Surface-expressed enolases of Plasmodium and other pathogens.* Mem Inst Oswaldo Cruz, 2011. **106 Suppl 1**: p. 85-90.

54. Pal-Bhowmick, I., et al., *Protective properties and surface localization of Plasmodium falciparum enolase.* Infect Immun, 2007. **75**(11): p. 5500-8.

55. Wu, Y., et al., *Phase 1 trial of malaria transmission blocking vaccine candidates Pfs25 and Pvs25 formulated with montanide ISA 51.* PLoS One, 2008. **3**(7): p. e2636.

56. Christophides, G.K. and A. Crisanti, *Vector and vector-borne disease research: need for coherence, vision and strategic planning.* Pathog Glob Health, 2013. **107**(8): p. 385-6.

57. Zhao, B., et al., *Regulation of the gut-specific carboxypeptidase: a study using the binary Gal4/UAS system in the mosquito Aedes aegypti.* Insect Biochem Mol Biol, 2014. **54**: p. 1-10.

58. Dinglasan, R.R., et al., *The Anopheles gambiae adult midgut peritrophic matrix proteome.* Insect Biochem Mol Biol, 2009. **39**(2): p. 125-34.

59. Gonzalez-Ceron, L., et al., *Bacteria in midguts of field-collected Anopheles albimanus block Plasmodium vivax sporogonic development.* J Med Entomol, 2003. **40**(3): p. 371-4.

60. Pumpuni, C.B., et al., *Bacterial population dynamics in three anopheline species: the impact on Plasmodium sporogonic development.* Am J Trop Med Hyg, 1996. **54**(2): p. 214-8.

61. Christophides, G.K., D. Vlachou, and F.C. Kafatos, *Comparative and functional genomics of the innate immune system in the malaria vector Anopheles gambiae.* Immunol Rev, 2004. **198**: p. 127-48.

62. Mead, E.A., et al., *Translational regulation of Anopheles gambiae mRNAs in the midgut during Plasmodium falciparum infection.* BMC Genomics, 2012. **13**: p. 366.

63. Richards, A.G., *The ultrastructure of the midgut of hematophagous insects.* Acta Trop, 1975. **32**(2): p. 83-95.

64. Shao, L., M. Devenport, and M. Jacobs-Lorena, *The peritrophic matrix of hematophagous insects.* Arch Insect Biochem Physiol, 2001. **47**(2): p. 119-25.

65. Toprak, U., et al., *Insect intestinal mucins and serine proteases associated with the peritrophic matrix from feeding, starved and moulting Mamestra configurata larvae.* Insect Mol Biol, 2010. **19**(2): p. 163-75.

66. Mosesson, M.W., *Fibrinogen and fibrin structure and functions.* J Thromb Haemost, 2005. **3**(8): p. 1894-904.

67. Fan, C., et al., *Fibrinogen-related protein from amphioxus Branchiostoma belcheri is a multivalent pattern recognition receptor with a bacteriolytic activity.* Mol Immunol, 2008. **45**(12): p. 3338-46.

68. Zhang, H., et al., *A fibrinogen-related protein from bay scallop Argopecten irradians involved in innate immunity as pattern recognition receptor.* Fish Shellfish Immunol, 2009. **26**(1): p. 56-64.

69. Wang, X., Q. Zhao, and B.M. Christensen, *Identification and characterization of the fibrinogen-like domain of fibrinogen-related proteins in the mosquito, Anopheles gambiae, and the fruitfly, Drosophila melanogaster, genomes.* BMC Genomics, 2005. **6**: p. 114.

70. Kawabata, S. and S. Iwanaga, *Role of lectins in the innate immunity of horseshoe crab.* Dev Comp Immunol, 1999. **23**(4-5): p. 391-400.

71. Wickham, T.J., et al., *Screening of insect cell lines for the production of recombinant proteins and infectious virus in the baculovirus expression system.* Biotechnol Prog, 1992. **8**(5): p. 391-6.

72. Invitrogen, *InsectSelect BSD system: for stable expression of heterologous proteins in lepidopteran insect cell lines using pIB/V5-His*. 2008, Invitrogen: Grand Island, NY. p. 1-31.

73. QIAGEN, *The QIAexpressionist: A handbook for high-level expression and purification of 6XHis-tagged proteins.* 2003, QIAGEN: Hilden, Germany. p. 1-128.

74. Duong-Ly, K.C. and S.B. Gabelli, *Gel filtration chromatography (size exclusion chromatography) of proteins.* Methods Enzymol, 2014. **541**: p. 105-14.

75. Jensen, J.B. and W. Trager, *Plasmodium falciparum in culture: use of outdated erthrocytes and description of the candle jar method.* J Parasitol, 1977. **63**(5): p. 883-6.

76. Beetsma, A.L., et al., *Plasmodium berghei ANKA: purification of large numbers of infectious gametocytes.* Exp Parasitol, 1998. **88**(1): p. 69-72.

77. Korochkina, S., et al., *A mosquito-specific protein family includes candidate receptors for malaria sporozoite invasion of salivary glands.* Cell Microbiol, 2006. **8**(1): p. 163-75.

78. Goodman, A.L., et al., *A viral vectored prime-boost immunization regime targeting the malaria Pfs25 antigen induces transmission-blocking activity.* PLoS One, 2011. **6**(12): p. e29428.

79. Li, J., J.M. Ribeiro, and G. Yan, *Allelic gene structure variations in Anopheles gambiae mosquitoes.* PLoS One, 2010. **5**(5): p. e10699.

80. Angrisano, F., et al., *Spatial localisation of actin filaments across developmental stages of the malaria parasite.* PLoS One, 2012. **7**(2): p. e32188.

81. Ploplis, V.A. and F.J. Castellino, *Nonfibrinolytic functions of plasminogen.* Methods, 2000. **21**(2): p. 103-10.

82. Povelones, M., et al., *The CLIP-domain serine protease homolog SPCLIP1 regulates complement recruitment to microbial surfaces in the malaria mosquito Anopheles gambiae.* PLoS Pathog, 2013. **9**(9): p. e1003623.

83. Povelones, M., et al., *Structure-function analysis of the Anopheles gambiae LRIM1/APL1C complex and its interaction with complement C3-like protein TEP1.* PLoS Pathog, 2011. **7**(4): p. e1002023.

84. Vega-Rodriguez, J., et al., *Multiple pathways for Plasmodium ookinete invasion of the mosquito midgut.* Proc Natl Acad Sci U S A, 2014. **111**(4): p. E492-500.

85. Han, Y.S., et al., *Molecular interactions between Anopheles stephensi midgut cells and Plasmodium berghei: the time bomb theory of ookinete invasion of mosquitoes.* EMBO J, 2000. **19**(22): p. 6030-40.

86. WHO, *World Malaria Report Summary* http://apps.who.int/iris/bitstream/10665/254912/1/WHO-HTM-GMP-2017.4-eng.pdf?ua=1, 2016.

87. Blobel, G. and B. Dobberstein, *Transfer of proteins across membranes. I. Presence of proteolytically processed and unprocessed nascent immunoglobulin light chains on membrane-bound ribosomes of murine myeloma.* J Cell Biol, 1975. **67**(3): p. 835-51.

88. Spielmann, T. and T.W. Gilberger, *Protein export in malaria parasites: do multiple export motifs add up to multiple export pathways?* Trends Parasitol, 2010. **26**(1): p. 6-10.

89. Patra, K.P. and J.M. Vinetz, *New ultrastructural analysis of the invasive apparatus of the Plasmodium ookinete.* Am J Trop Med Hyg, 2012. **87**(3): p. 412-7.

90. Saxena, A.K., Y. Wu, and D.N. Garboczi, *Plasmodium p25 and p28 surface proteins: potential transmission-blocking vaccines.* Eukaryot Cell, 2007. **6**(8): p. 1260-5.

91. Li, F., et al., *Apical surface expression of aspartic protease Plasmepsin 4, a potential transmission-blocking target of the plasmodium ookinete.* J Biol Chem, 2010. **285**(11): p. 8076-83.

92. Invitrogen. *Bac-to-Bac® Baculovirus Expression System* 2015; Available from: https://tools.thermofisher.com/content/sfs/manuals/bactobac_man.pdf.

93. Katris, N.J., et al., *The apical complex provides a regulated gateway for secretion of invasion factors in Toxoplasma.* PLoS Pathog, 2014. **10**(4): p. e1004074.

94. Yoshida, S., et al., *Plasmodium berghei circumvents immune responses induced by merozoite surface protein 1- and apical membrane antigen 1-based vaccines.* PLoS One, 2010. **5**(10): p. e13727.

95. Alaro, J.R., et al., *A chimeric Plasmodium falciparum merozoite surface protein vaccine induces high titers of parasite growth inhibitory antibodies.* Infect Immun, 2013. **81**(10): p. 3843-54.

96. Burns, J.M., Jr., et al., *Immunogenicity of a chimeric Plasmodium falciparum merozoite surface protein vaccine in Aotus monkeys.* Malar J, 2016. **15**: p. 159.

97. Sheikh, I.H., et al., *Immunogenicity of a plasmid DNA vaccine encoding 42kDa fragment of Plasmodium vivax merozoite surface protein-1.* Acta Trop, 2016. **162**: p. 66-74.

98. Neal, A.T., et al., *Limited variation in vaccine candidate Plasmodium falciparum Merozoite Surface Protein-6 over multiple transmission seasons.* Malar J, 2010. **9**: p. 138.

99. Bozdech, Z., S. Mok, and A.P. Gupta, *DNA microarray-based genome-wide analyses of Plasmodium parasites.* Methods Mol Biol, 2013. **923**: p. 189-211.

100. Nguyen-Duc, T., et al., *Nanobody(R)-based chromatin immunoprecipitation/micro-array analysis for genome-wide identification of transcription factor DNA binding sites.* Nucleic Acids Res, 2013. **41**(5): p. e59.

101. Zhu, H., et al., *Analysis of yeast protein kinases using protein chips.* Nat Genet, 2000. **26**(3): p. 283-9.

102. Zhu, H., et al., *Global analysis of protein activities using proteome chips.* Science, 2001. **293**(5537): p. 2101-5.

103. Hall, D.A., et al., *Regulation of gene expression by a metabolic enzyme.* Science, 2004. **306**(5695): p. 482-4.

104. Jones, R.B., et al., *A quantitative protein interaction network for the ErbB receptors using protein microarrays.* Nature, 2006. **439**(7073): p. 168-74.

105. Michaud, G.A., et al., *Analyzing antibody specificity with whole proteome microarrays.* Nat Biotechnol, 2003. **21**(12): p. 1509-12.

106. Giraldo-Calderon, G.I., et al., *VectorBase: an updated bioinformatics resource for invertebrate vectors and other organisms related with human diseases.* Nucleic Acids Res, 2015. **43**(Database issue): p. D707-13.

107. Baker, D.A., et al., *A comprehensive gene expression atlas of sex- and tissue-specificity in the malaria vector, Anopheles gambiae.* BMC Genomics, 2011. **12**: p. 296.

108. Marinotti, O., et al., *Genome-wide analysis of gene expression in adult Anopheles gambiae.* Insect Mol Biol, 2006. **15**(1): p. 1-12.

109. Lowenberger, C.A., et al., *Mosquito-Plasmodium interactions in response to immune activation of the vector.* Exp Parasitol, 1999. **91**(1): p. 59-69.

110. Bradford, M.M., *A rapid and sensitive method for the quantitation of microgram quantities of protein utilizing the principle of protein-dye binding.* Anal Biochem, 1976. **72**: p. 248-54.

111. Huang, X., et al., *Drosophila Niemann-Pick type C-2 genes control sterol homeostasis and steroid biosynthesis: a model of human neurodegenerative disease.* Development, 2007. **134**(20): p. 3733-42.

112. Behmer, S.T. and W.D. Nes, *Insect sterol nutrition and physiology: A global overview.* Advances in Insect Physiology, Vol 31, 2003. **31**: p. 1-72.

113. Wu, D.D., D.M. Irwin, and Y.P. Zhang, *Molecular evolution of the keratin associated protein gene family in mammals, role in the evolution of mammalian hair.* BMC Evol Biol, 2008. **8**: p. 241.

114. Heo, K., et al., *Involvement of Niemann-Pick type C2 protein in hematopoiesis regulation.* Stem Cells, 2006. **24**(6): p. 1549-55.

115. Storch, J. and Z. Xu, *Niemann-Pick C2 (NPC2) and intracellular cholesterol trafficking.* Biochim Biophys Acta, 2009. **1791**(7): p. 671-8.

116. Schonbrunn, E., et al., *Interaction of the herbicide glyphosate with its target enzyme 5-enolpyruvylshikimate 3-phosphate synthase in atomic detail.* Proc Natl Acad Sci U S A, 2001. **98**(4): p. 1376-80.

117. Sherman, I.W., *Amino acid metabolism and protein synthesis in malarial parasites.* Bull World Health Organ, 1977. **55**(2-3): p. 265-76.

Appendix

Table of *An. gambiae* Midgut Proteins that Potentially Interact with *P. falciparum* Parasites.

#	Vectorbase Gene ID	Omics Gene ID	Predicted Functions
1	AGAP003781-PA	6161	amylase
2	AGAP012263-PA	9055	amylase
3	AGAP009102-PA	10764	amylase
4	AGAP000862-PA	14156	amylase
5	AGAP006268-PA	1663	chitin
6	AGAP001203-PA	3197	chitin binding
7	AGAP001005-PA	14321	chitin binding
8	AGAP007016-PA	2412	Deaminase
9	AGAP011476-PA	8202	defense
10	AGAP005416-PA	742	defense
11	AGAP006425-PA	1794	defense
12	AGAP007197-PA	2608	defense
13	AGAP001956-PA	4007	defense
14	AGAP002796-PA	5011	defense
15	AGAP002848-PA	5070	defense
16	AGAP002870-PA	5092	defense
17	AGAP011325-PA	8009	defense
18	AGAP001873-PA	10494	defense
19	AGAP004632-PA	16151	defense
20	AGAP007182-PA	2593	egg production
21	AGAP007672-PA	3066	lipase
22	AGAP009101-PA	10761	lipase
23	AGAP010820-PA	14774	lipase
24	AGAP003573-PA	5915	lipid binding
25	AGAP013327-PA	7447	peroxidase
26	AGAP008398-PA	9923	pheromone
27	AGAP004054-PA	6449	phophatase
28	AGAP006400-PA	1764	phosphatase
29	AGAP008487-PA	10035	phosphatase
30	AGAP007140-PA	2551	phosphatase and nucleotase
31	AGAP007677-PA	3070	protease
32	AGAP005686-PA	1019	protease
33	AGAP005691-PA	1024	protease
34	AGAP006534-PB	1027	protease
35	AGAP006144-PA	1531	protease
36	AGAP006210-PA	1595	protease

37	AGAP007262-PA	2674	protease
38	AGAP001245-PA	3253	protease
39	AGAP013377-PA	3662	protease
40	AGAP013155-PA	3930	protease
41	AGAP005093-PA	4785	protease
42	AGAP011434-PA	8151	protease
43	AGAP011442-PA	8160	protease
44	AGAP011908-PA	8664	protease
45	AGAP011920-PA	8680	protease
46	AGAP008176-PA	9685	protease
47	AGAP008999-PA	10642	protease
48	AGAP000476-PA	13675	protease
49	AGAP004900-PA	15223	protease
50	AGAP013078-PA	15853	protease
51	AGAP011379-PA	8079	signal transduction
52	AGAP006972-PA	2367	structural
53	AGAP001509-PA	3536	structural
54	AGAP008463-PA	12734	structural
55	AGAP005795-PA	1149	transport
56	AGAP004323-PA	5418	transport
57	AGAP002094-PA	4180	transport
58	AGAP013451-PA	4760	lipid binding
59	AGAP004367-PA	17225	transport
60	AGAP001183-PA	3169	UMP hydrolase
61	AGAP008678-PA	10230	unknown
62	AGAP006484-PA	1864	unknown
63	AGAP001508-PA	3535	unknown
64	AGAP011006-PA	7653	unknown
65	AGAP008138-PA	9641	unknown
66	AGAP005899-PA	1268	unknown
67	AGAP006256-PA	1646	unknown
68	AGAP007077-PA	2486	unknown
69	AGAP007370-PA	2775	unknown
70	AGAP007564-PA	2945	unknown
71	AGAP007606-PA	2994	unknown
72	AGAP001171-PA	3156	unknown
73	AGAP002577-PA	4740	unknown
74	AGAP002974-PA	5229	unknown
75	AGAP003010-PA	5273	unknown
76	AGAP003255-PA	5555	unknown
77	AGAP003499-PA	5832	unknown

78	AGAP004035-PA	6433	unknown
79	AGAP004303-PA	6737	unknown
80	AGAP011371-PA	8071	unknown
81	AGAP011378-PA	8077	unknown
82	AGAP011646-PA	8387	unknown
83	AGAP007924-PA	9434	unknown
84	AGAP008190-PA	9700	unknown
85	AGAP009240-PA	10924	unknown
86	AGAP009805-PK	11565	unknown
87	AGAP001608-PA	11610	unknown
88	AGAP010151-PA	11879	unknown
89	AGAP000014-PA	13104	unknown
90	AGAP000168-PA	13288	unknown
91	AGAP000307-PA	13471	unknown
92	AGAP000550-PA	13778	unknown
93	AGAP008670-PA	4788	unknown
94	AGAP008552-PA	10104	unknown
95	AGAP007031-PA	2434	FREP1

Copyright Permission Letter from the *Journal of Biological Chemistry*.

11200 Rockville Pike
Suite 302
Rockville, Maryland 20852

August 19, 2011

American Society for Biochemistry and Molecular Biology

To whom it may concern,

It is the policy of the American Society for Biochemistry and Molecular Biology to allow reuse of any material published in its journals (the Journal of Biological Chemistry, Molecular & Cellular Proteomics and the Journal of Lipid Research) in a thesis or dissertation at no cost and with no explicit permission needed. Please see our copyright permissions page on the journal site for more information.

Best wishes,

Sarah Crespi

American Society for Biochemistry and Molecular Biology
11200 Rockville Pike, Rockville, MD
Suite 302
240-283-6616
JBC | MCP | JLR

Tel: 240-283-6600 • Fax: 240-881-2080 • E-mail: asbmb@asbmb.org